R. & M. No. 3156
(20,459) (20,460) (20,461)
A.R.C. Technical Report

R. & M. No. 3156

MINISTRY OF AVIATION

AERONAUTICAL RESEARCH COUNCIL
REPORTS AND MEMORANDA

Review and Extension of Transonic Aerofoil Theory

Part I.—Introduction and Qualitative Analysis
Part II.—Analysis of Measured Pressure Distributions
Part III.—Analysis of Theoretical Solutions

By C. S. SINNOTT, B.Sc., Ph.D., and J. OSBORNE, B.Sc.
of the AERODYNAMICS DIVISION, N.P.L.

LONDON: HER MAJESTY'S STATIONERY OFFICE
1961
PRICE 18*s.* 0*d.* NET

Review and Extension of Transonic Aerofoil Theory

Parts I to III

By C. S. SINNOTT, B.Sc., Ph.D., and J. OSBORNE, B.Sc.
of the AERODYNAMICS DIVISION, N.P.L.

*Reports and Memoranda No. 3156**
October, 1958

Summary. Part I is an introduction to an empirical and theoretical study of two-dimensional aerofoil flows which include a limited region of supersonic flow terminated by a shock wave. A brief review of theoretical studies of the problem is followed by a detailed analysis of the flow pattern and associated pressure distribution. A scheme for the analysis of measured pressure distributions is thus derived, and this is used in Part II of the present paper to construct a semi-empirical method for the estimation of pressure distributions. The implications of the results established by this analysis are discussed in relation to the development of transonic aerofoil flows. In Part III the results of an integral solution of the transonic flow equation are examined, and modified on the basis of the analysis of Part II.

PART I

INTRODUCTION AND QUALITATIVE ANALYSIS

1.1. *Introduction.* Theoretical methods for the estimation of the two-dimensional inviscid flow about aerofoil sections have existed for many years. The incompressible flow about simple profiles can be calculated exactly, and useful approximate solutions for the compressible subsonic flow about geometrically defined profiles have been developed. However, in these compressible-flow methods a solution is obtained only by recourse to approximations to the governing equation which destroy the feature that is essential for the representation of mixed subsonic/supersonic flows, *i.e.*, the change from an elliptic form to a hyperbolic form of the equation when the local speed passes from below to above the local speed of sound. This change in form is associated with a non-linear term in the equation, which if retained leads to great difficulties in the derivation of an analytical solution to even the most simple transonic flows; in this paper an alternative approach is suggested. This approach is based on approximations that appear sensible from the physics of the flow, rather than to facilitate a mathematical analysis of the flow equations.

The flow over an aerofoil surface in which a local region of supersonic flow terminated by a shock wave occurs is of great importance. A large volume of experimental data for this type of flow has been obtained, and it has been found that the development of supersonic-flow regions leads to

* Published with the permission of the Director, National Physical Laboratory.

significant modifications to the form of the pressure distribution over an aerofoil. One result is an increase in pressure drag due to the development of a low-pressure supersonic region behind the crest of the aerofoil surface. It is in this way the energy losses through the shock wave which terminates the supersonic flow are transmitted to the aerofoil surface. Measured pressure distributions of this type are shown in Fig. 1. A feature of transonic aerofoil flows of equal or greater importance is the effect on the boundary layer of the rapid pressure rise through the shock wave. With quite moderate shock pressure rises this can lead to separation of the boundary layer and hence to severe changes in loading, with the consequences described in Ref. 1. The inherent instability of the separated flow results in unsteady phenomena in flight such as buffeting. The study of shock-induced boundary-layer separation, and methods of avoidance or prevention, has been a major aim of high-subsonic experimental work.

Recently further consideration has been given to the design of aerofoil sections to operate at high-subsonic speeds. It has been suggested that it may be advantageous to design for pressure distributions which include limited supersonic regions. To achieve useful gains this requires that no significant loss of leading-edge suction occurs, and that the shock wave terminating the local supersonic flow forms in the neighbourhood of the aerofoil surface crest, and is not strong enough to induce boundary-layer separation. To take advantage of these possibilities and also to assess aerofoil characteristics in off-design conditions, a knowledge of the factors which affect shock-wave movement and strength is desirable.

The objects of the investigations described in this series of papers are to assess the usefulness of existing theoretical methods for the prediction of transonic pressure distributions, and to suggest improvements, and to analyse transonic experimental data to establish an alternative empirical method for the prediction of pressure distributions. It is then shown how theoretical methods might be improved by the use of the empirical relations established.

A brief review of theoretical methods for the estimation of mixed subsonic/supersonic flows is given below, and in Section 1.3 a discussion of the flow pattern and associated pressure distribution is given. This is followed by an outline of the approach used in Part II for the analysis of measured transonic pressure distributions. Part II also includes a discussion of the physical mechanism governing some aspects of the development of transonic flows, based on the results of the analysis. Part III contains a summary of the most promising analytical method, a discussion of solutions that have been calculated, and the relation of these to the results of Part II.

1.2. *Theoretical Methods.* Many mathematical studies of transonic flow have considered the flow of a sonic stream past a simple aerofoil section. In this problem a shock wave occurs only at the trailing edge of the profiles considered and need not be treated explicitly in solutions for the pressure distribution over the profile. The methods chiefly used in the analyses are transformation to the hodograph plane and the method of characteristics. Hodograph solutions cannot be easily obtained for arbitrary geometric boundaries, and have mainly been used to study the flow past flat-plate and wedge profiles. The method of characteristics can be used to calculate supersonic-flow development about curved surfaces, but requires a knowledge of the sonic line (or some other supersonic-pressure boundary) as a starting point in the calculation. However, the determination of this itself requires the analysis of a mixed flow region. Neither of these approaches is suitable for the estimation of transonic flows about round-nosed aerofoil sections, even with a free-stream Mach number of unity, though useful solutions have been obtained for simple profiles; these are discussed

in Ref. 2. Mathematical methods directly related to the calculation of transonic flows with high-subsonic free-stream conditions and arbitrary aerofoil profiles are considered below.

The shock waves which may occur in the flow of a high-subsonic stream about an aerofoil are usually not strong enough to invalidate significantly the assumption that the flow is irrotational and isentropic. It is thus permissible to consider a velocity potential Φ, and it can be shown that for two-dimensional flows Φ must satisfy the following equation

$$(a^2 - \Phi_x^2)\Phi_{xx} + (a^2 - \Phi_y^2)\Phi_{yy} - 2\Phi_x\Phi_y\Phi_{xy} = 0. \tag{1}$$

Suffices denote partial derivatives; the local speed of sound, a, is a function of the free-stream parameters, and Φ_x and Φ_y. It is convenient to introduce a perturbation velocity potential ϕ, where

$$\phi = \Phi - U_0 x.$$

If the usual thin-wing-theory assumptions are made, and terms higher than the second order neglected, equation (1) becomes

$$(1 - M_0^2)\phi_{xx} + \phi_{yy} = \frac{M_0^2}{U_0}\left[\phi_x\{(\gamma + 1)\phi_{xx} + (\gamma - 1)\phi_{yy}\}\right]. \tag{2}$$

To represent the particular feature of transonic flow it is only necessary to retain the terms in $\phi_x\phi_{xx}$ of the right-hand side of equation (2), leaving

$$(1 - M_0^2)\phi_{xx} + \phi_{yy} = M_0^2\frac{\gamma + 1}{U_0}\phi_x\phi_{xx}. \tag{3}$$

Minor differences in the perturbation analysis can lead to different expressions for the coefficient of the non-linear term in equation (3), a point which is discussed in detail in Ref. 3.

Even in the much reduced form given by equation (3) the compressible-flow equation is not amenable to direct analytical treatment. Moreover, equation (3) is only valid in regions where the necessary derivatives are continuous; therefore if shock waves are to be considered a further relation is necessary. It is also of course necessary that a solution must satisfy the boundary conditions of a given flow.

An alternative derivation of the exact compressible-flow equation is given in Ref. 4 and is possibly a more useful form to that given above for the application of numerical methods.

Two distinct approaches to the solution of the non-linear partial differential equation for the flow about aerofoils have been adopted. Attempts have been made to calculate solutions of the exact equation by using the methods of numerical analysis, notably relaxation. References 4 and 5 are examples of this approach, neither of which appears wholly satisfactory. Emmons's[6] (1946) earlier work has, however, been extremely valuable in throwing light on the flow in the neighbourhood of a normal shock wave adjacent to a solid boundary. A serious drawback in attempts to derive solutions to the exact equation is the amount of computation required. It is possible that useful results could be obtained if electronic computors can be used to perform the relaxation process.

The alternative approach to the calculation of transonic flows is that based on approximations to the equation to facilitate the use of analytical methods. It is essential in this approach that the mixed elliptic/hyperbolic nature of the equation is retained. Approximations introduced to linearize the equation, or to reduce it to a set of linear equations do not give a proper representation of the significant differences in stream-tube behaviour in subsonic and supersonic flow. The well-known methods of expressing the velocity potential as an expansion in Mach number or aerofoil thickness

are of this kind, and although they lead to solutions which include local supersonic regions, they are physically unreal. The same criterion applies to the method of solution of the transonic-flow equations suggested by Meksyn[7] (1953) (*see* Ref. 8); it is interesting to note that this method is shown to be equivalent to the M^2 expansion method by Imai[9] (1957).

An analytical solution of a simplified form of the transonic-flow equation in which the essential quadratic nature of the equation is retained has been developed by Spreiter and Alksne[8] (1955); the analysis follows that of Oswatitsch[10] (1950) and Gullstrand[11] (1952). The differential equation governing the flow is converted into an integral equation to which an iterative solution is obtained. Solutions for mixed subsonic/supersonic flows including shock waves can be obtained, but approximations introduced to simplify the analysis and computation still prevent an exact representation of the physics, particularly in the neighbourhood of a shock wave. However, Spreiter's method appears to be by far the most promising theoretical approach to transonic-flow problems, and the analysis of results obtained by a modified form of it is the basis of Part III of the present paper.

1.3. *Features of the Transonic Flow about an Aerofoil.* The type of flow considered is that for which the free-stream Mach number is such that the flow over part of the aerofoil surface is supersonic. When the maximum local Mach number exceeds about $1 \cdot 10$ it appears that the downstream boundary conditions can only be satisfied in a real viscous flow by the termination of the supersonic region by an abrupt pressure rise to subsonic conditions. Although this type of flow is certainly a possible theoretical inviscid flow, no entirely satisfactory explanation of its predominance over the sometimes possible smooth supersonic deceleration has yet been found; a number of interesting hypotheses are discussed in Ref. 12. If mixed subsonic/supersonic shock-free flows can be shown to be inherently unstable, the presence of a boundary layer in real flows could well provide a triggering mechanism to induce collapse into discontinuous flow. In this paper it is supposed that all limited supersonic regions terminate in shock waves. The shock-wave position must then be such that the pressure on the aerofoil surface immediately upstream of the shock (p_1), and that immediately downstream (p_2), which must be related *via* the flow over the rear of the aerofoil and the wake to the downstream boundary conditions, are such that the ratio p_2/p_1 satisfies a consistent relation. This condition is discussed in detail in Section 1.3.2.

The flow of a high subsonic stream past an aerofoil is illustrated in Fig. 2a, and the associated pressure distribution in Fig. 2b. The upper-surface flow is of the mixed subsonic/supersonic type, including a shock wave, considered in this paper. Discussion of this flow can conveniently be divided into three parts; the subsonic and supersonic region upstream of the shock wave, the shock wave, and the subsonic flow downstream of the shock wave.

1.3.1. *Flow upstream of shock wave.* A typical family of pressure distributions with free-stream Mach number (M_0) as parameter is shown in Fig. 1. It is seen that once a region of supersonic flow has developed further increase in M_0 leads to a downstream movement of the shock wave and extension of the supersonic-flow region, but to only small changes in local pressure ahead of the shocks*. This is the well-known 'Mach number freeze' phenomenon discussed in Ref. 2. It is shown in that paper that the pressure distribution over an aerofoil surface at $M_0 = 1$ can be related to the surface slope and to the leading-edge geometry, for these determine the sonic-line shape and

* For an aerofoil at incidence there may be large changes in pressure near the leading edge with changes in M_0 over a limited range above the critical Mach number.

following supersonic-flow development. For high subsonic values of M_0 the development of the supersonic region must also be determined by these parameters, as is evidenced by the occurrence of the Mach-number freeze. It therefore seems reasonable to attempt to relate supersonic flow occurring at high-subsonic speeds to the corresponding 'sonic-range' flow. The introduction of some parameter to account for changes in sonic-line shape will clearly be necessary, as will the representation of the overall flow field about different aerofoils, as this is subsonic. The analysis of measured local supersonic pressure distributions in Part II is based on this approach.

1.3.2. *Shock pressure rise.* It is noted above that the pressures immediately upstream and downstream of a shock wave must be related in some consistent manner. This relation can be shown, by analysis of the stream tube adjacent to the surface, to be the classical normal-shock pressure-rise equation*. Now in addition to the complexity of the transonic-flow equation discussed in Section 1.2, a further problem in the correlation of theoretical and experimental studies of transonic flow is the finding that measured shock pressure rises are invariably less than those given by the shock equation. Moreover, as some typical results given in Fig. 5 show, they are not found to follow any definite trend. Fortunately the detailed numerical solutions for mixed flows in a hyperbolic nozzle obtained by Emmons[6] suggest an explanation of the discrepancies. Emmons found that if he used the normal shock equation to determine the pressure change through a shock, the predicted pressure rise was followed immediately by a pressure fall. He explains this behaviour by considering the effect on the pressure gradient normal to the surface of applying the shock relation along a line normal to the streamlines. It is clear that a reversal in direction of the normal pressure gradient must occur, and hence there must be a discontinuity in surface curvature at the shock position. This discontinuity in surface, or more correctly, bounding streamline curvature, would be expected to lead to a local pressure fall in a manner analogous to the incompressible flow over a curvature singularity. In the inviscid-flow problem postulated by Emmons, the pressure changes were found to occur in a very small region and led to solutions in which the shock pressure rise appeared to be less than that given by classical theory. From the analogy with the incompressible flow past a boundary curvature singularity the streamwise extent of the pressure changes would be expected to depend on the strength of the singularity, which is dependent on the Mach number ahead of the shock and the local surface curvature. In a viscous flow the phenomenon will clearly be associated with a local thickening or separation of the boundary layer, and is further complicated by the influence of the rapid pressure change itself on the equilibrium of the boundary layer.

This aspect of shock-wave boundary-layer interaction has been studied by Gadd[13] (1957). He shows that a local increase in boundary-layer displacement thickness under the influence of the shock pressure rise leads to an effective decrease in stream-tube cross-section near the surface and hence, with local subsonic flow, to a pressure fall. However, this mechanism is effective over a few boundary-layer thicknesses only. Neither it, nor the previous hypothesis, explains the non-attainment of the full normal shock pressure rise for a shock on a surface with zero curvature, as on the wedge tail of many aerofoil sections. In such cases the existence of non-uniform flow normal to the surface above the surface may influence the pressure changes behind the shock wave.

A further feature of transonic shock-wave boundary interaction follows from Emmons's analysis. For very weak shock waves the pressure fall following a shock was found to lead to the establishment

* Which states that p_2/p_1 is a function of M_1 only.

of supersonic flow, the shock pressure-rise–pressure-fall pattern was then repeated, possibly many times. The sketch below shows the type of pressure distribution associated with this phenomenon.

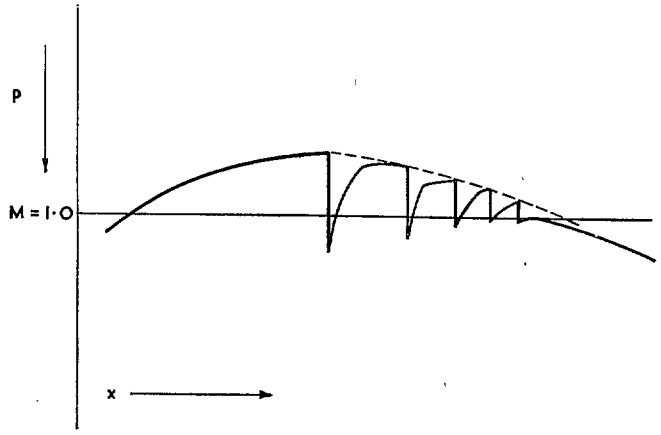

The broken line indicates the pressure distribution that would be deduced for a flow of this nature by interpolation from relatively widely spaced pressure measurements, as in the analysis of wind-tunnel tests. The presence of a boundary layer would also be expected to obscure the details of the corresponding inviscid-flow pressure distribution. Earlier it is noted that shock waves are detected in such tests when the maximum local Mach number exceeds about 1·1. It may well be that repeated shocks of the kind sketched above occur at lower Mach numbers, and that the apparent upper limit for shock-free flows is an upper limit for these repeated shocks. Emmons's calculations for the flow through a nozzle gave a corresponding local Mach-number limit of 1·075.

1.3.3. *Flow downstream of shock wave.* Downstream of a shock wave the pressure changes must satisfy the boundary conditions imposed by the geometry of the surface, boundary layer and wake, and in particular the flow must return to the initial free-stream conditions downstream.

It is well known that for wholly subsonic flows the pressure distribution over an aerofoil at different free-stream Mach numbers can be related by simple compressibility formulae. A significant development of this type of Mach number variation is its continuation in part to flows which include a region of supersonic flow terminating in a shock wave. It is found that the pressure distribution some distance downstream of a shock can be approximately estimated from that in a wholly subsonic flow in the same way. This is noticeable for both measured and calculated transonic pressure distributions. A possible explanation of the phenomenon is given in Section 5 of Part II.

1.4. *Basic Method for Constructing Transonic Pressure Distributions.* The analysis of mixed subsonic/supersonic pressure distributions in Section 1.3 suggests that the estimation of pressure distributions might be usefully approached in the three stages considered. For a given aerofoil the sonic-range pressure distribution can be used as a first approximation to the supersonic distribution in flows with shock waves upstream of the trailing edge. This $M_0 = 1{\cdot}0$ distribution would then represent the locus of pressures immediately upstream of shock waves occurring at lower Mach numbers. Also, if it is assumed that the simple variation of the subsonic pressures near the trailing edge discussed above, can be extended upstream to the shock positions, then a family of distributions, dependent on M_0, can be estimated. This position is summarised in Fig. 3a. To determine the pressure distribution for a given shock position (or given M_0) the appropriate shock pressure-rise

relation is required, for this, together with the assumed p_1 locus, will define a p_2 locus. The intersections of the p_2 locus with the members of the shock-free flow family, then gives the shock movement with free-stream Mach number and the associated pressure distributions. Results obtained by the above scheme are shown in Fig. 3b. Here the classical normal-shock pressure-rise equation has been used to derive the p_2 locus from the sonic-range pressure distribution calculated by the method of Ref. 5. The shock-free flow family of downstream pressure distributions were calculated from the measured distribution at $M_0 = 0{\cdot}70$ by the Glauert compressibility rule.

An analysis on these lines might give an indication of the rate of change of shock movement with free-stream Mach number. However, the comparison of shock positions given in Fig. 4 shows that pressure distributions estimated in this way are of little value: reference to Fig. 1 also shows that the $M_0 = 1{\cdot}0$ distribution is but a poor approximation to the supersonic flow at lower Mach numbers. The cause of the large differences in shock position for a given Mach number is evident in the comparison of the assumed (exact normal-shock equation) and measured shock pressure-rise ratios shown in Fig. 5. It is clearly necessary to establish a shock pressure-rise relation which includes the effects of non-uniform flow normal to the aerofoil surface and of shock-wave boundary-layer interaction discussed in Section 1.3.2. The major part of the analysis of Part II is directed towards this end. It is also shown in Part II that an improved method for the estimation of supersonic-flow regions can be derived.

1.5. *Concluding Remarks.* This introductory Section describes the development of mixed subsonic/supersonic flows, and discusses a possible approach to the analysis of measured pressure distributions. The ideas of Sections 1.3 and 1.4 are used in Part II as a guide to the analysis of a large volume of two-dimensional aerofoil data. A method for the prediction of pressure distributions which include shock waves is derived and shown to give usefully accurate results. The empirical relations established by the analysis are considered in relation to the physical mechanism governing the development of transonic flows, and a close link with the corresponding shock-free flow is suggested. In Part III of the present series of papers solutions calculated by the theoretical method of Ref. 3 are compared with experiment. It is shown how the poor physical representation of certain features of transonic flow inherent in the theory lead to large discrepancies from experimental results. Replacement of part of the theoretical solution by results of the empirical analysis of Part II is shown to give much improved correlation with experiment. It is suggested how these modifications may be included in the theoretical representation of the flow so that improved solutions may be obtained by direct calculation.

One aim of this study of transonic pressure distributions over aerofoils was the desire to gain an insight into the factors affecting aerofoil characteristics at high subsonic speeds; particularly those related to the onset of the transonic drag-rise and of shock-induced boundary-layer separation. The transonic drag-rise is due not only to the development of a low-pressure region on the rearward facing part of an aerofoil surface, but also to the loss of leading-edge suction. This arises partly from the local Mach-number freeze over the forward part of an aerofoil when a supersonic-flow region has developed, and partly from the forward movement of the stagnation point if the aerofoil is at incidence. The present methods of calculating pressure distributions are only relevant when the conception of a Mach-number freeze is approximately true over all or nearly all the aerofoil chord, and therefore the influence of the leading-edge flow on the drag-rise cannot be estimated. The method should, however, prove valuable in the assessment of the onset of shock-induced separation. Existing

criteria for the onset of separation are based on two different interpretations of shock strength, the shock pressure-rise ratio and the upstream pressure. That based on pressure ratio, p_2/p_1, will clearly need to be redefined in terms of the convention for p_2 used in the present analysis. However, the analysis of Part II leads directly to values for shock upstream pressure, so that methods for the prediction of the onset of separation based on critical values of this quantity should be directly relevant.

Although no method of design for a desired form of transonic pressure distribution can be suggested, it is possible to compare properties of alternative aerofoil sections, and to assess the importance of particular geometrical features, by use of the present analysis. These problems are closely related to that of estimating the flow characteristics mentioned above, and will be considered in a later paper on applications of the present scheme for the prediction of transonic pressure distributions.

NOTATION

a	Local speed of sound
c	Aerofoil chord
H_0	Free-stream stagnation pressure
M	Mach number
M_0	Free-stream Mach number
p	Static pressure
p_1, p_2	Static pressure immediately upstream and downstream of a shock wave respectively
U_0	Free-stream speed
x, y	Cartesian co-ordinates, x in direction of free-stream velocity
γ	Ratio of specific heats
ϕ, Φ	Velocity potentials

PART II

ANALYSIS OF MEASURED PRESSURE DISTRIBUTIONS

2.1. *Introduction.* A method for the prediction of two-dimensional aerofoil pressure distributions which include a region of supersonic flow terminated by a shock wave is derived from an analysis of measured pressure distributions. The basis of the analysis is described in Part I. It is suggested there that a transonic pressure distribution may be usefully considered as divided into three parts: that ahead of the shock wave, the shock pressure rise, and that downstream of the shock wave. Quantitative features of these regions are correlated with known flows and with representative parameters of the overall flow about an aerofoil.

In Part I it is noted that the sonic-range pressure distribution over an aerofoil surface may be taken as a first approximation to the supersonic part of the pressure distribution at lower Mach numbers. Indeed the similarity in form of supersonic distributions at high subsonic speeds to that at $M_0 = 1$ suggests that the effects of aerofoil shape are well represented by the $M_0 = 1$ distribution; effects of free-stream Mach number and of the overall flow pattern would then be expected to determine differences in magnitude. This approach is adopted for the analysis of the supersonic part of transonic pressure distributions. Firstly, an analysis is made of differences between the pressure immediately upstream of shock waves, p_1, and the corresponding sonic-range value, and an empirical relation is established. This is followed by a similar analysis for the pressure difference at the crest of aerofoil surfaces. It is then found that linear interpolation between the pressure differences at crest and shock position leads to a good estimate of the supersonic pressure distribution in this region. The analysis for $(p_1 - p_{SR})/H_0$ and $(p_{CR} - p_{SR})/H_0$ is described in Section 2.2.1.

It is emphasised in Part I that discrepancies between measured shock pressure-rise ratios and the classical normal-shock equation is one of the most disturbing features in attempts to predict transonic pressure distributions. Although Emmons[6] (1946) has suggested a physical mechanism which can account for these differences, the additional direct effects of shock-wave boundary-layer interaction appear to frustrate any attempt to relate this mechanism to observed flows. Shock pressure rises obtained from wind-tunnel tests are difficult to define accurately, and appear sensitive to the test conditions. Therefore before an analysis of experimental results could be undertaken it was essential to choose a consistent method of interpreting the data. The relation between the pressure distribution over an aerofoil surface downstream of a shock wave to the corresponding low-speed flow discussed in Part I, Section 1.3.3, suggests a possible approach to this problem. It is shown in Ref. 14 that the Prandtl-Glauert rule gives the best representation of this type of flow behaviour near the trailing-edge, and this simple rule is used to define the pressure immediately downstream of observed shock waves. That is, in the analysis of wind-tunnel results the pressure immediately downstream of the shock waves is defined as the value predicted at that position by the Glauert compressibility formula (applied to results for some lower Mach number) for the Mach number corresponding to the observed shock position; this pressure is denoted p_{2G}. This convention is regarded as a means of interpolating in the neighbourhood of the shock wave in a consistent manner. To ensure consistency only results which follow the Glauert compressibility variation at least at the trailing edge are used in the analysis*.

As would be expected, in all but a few of the examples considered p_{2G} differs from the measured,

* In Section 2.5.2 it is shown that useful results can be obtained in cases where this condition is not satisfied.

or more correctly, estimated values of p_2, and it has not been possible to relate the differences to any flow or aerofoil parameter. However, it is shown in Section 2.2.2 that p_{2G}/p_1 can be directly related to p_1/H_0 to give a relation qualitatively similar to the classical normal-shock relation. The significance of this result in relation to the establishment of transonic flows is discussed in Section 2.5.1.

The usefulness of simple compressibility formulae for estimating the pressure distribution downstream of a shock wave is considered in detail in Ref. 14; results so obtained are illustrated by the examples of the application of the scheme for predicting transonic pressure distributions discussed later.

The next Section describes the analysis of measured pressure distributions, and the empirical relationships established from this analysis. The significance of these results in relation to the development of transonic flows and to theoretical methods is discussed in Section 2.5.1 and in Part III of the present paper. In Section 2.3 a scheme for the calculation of mixed subsonic/supersonic pressure distributions based on the empirical relations is described. Results are obtained for a number of examples, and the accuracy and applicability of the method is discussed in Section 2.5.2. Details of the experimental results used are given in Section 2.4.

2.2. *Analysis of Measured Pressure Distributions.* 2.2.1. *Supersonic region.* Theoretical and experimental studies of transonic flow have shown that the rate of change with free-stream Mach number of the local supersonic pressure distribution over an aerofoil surface is small for free-stream Mach numbers near one. The typical families of measured pressure distributions of Figs. 6 to 9 illustrate that the supersonic pressure distributions are in consequence similar in form to the corresponding sonic-range (or $M_0 = 1{\cdot}0$) pressure distribution. Analysis of this part of transonic pressure distributions has therefore been based on the study of the differences between local pressure at high-subsonic values of M_0 and that at the same chordwise position at $M_0 = 1{\cdot}0$.

A prime requirement of the present scheme for the prediction of pressure distributions is the estimation of the pressure immediately upstream of a shock wave, p_1. As suggested above it is supposed that the major flow and geometrical parameters which determine this are included in the sonic-range distribution so that the analysis can be restricted to the pressure (ratio) difference $(p_1 - p_{SR})/H_0$. Values of this quantity obtained from a wide range of wind-tunnel tests are shown plotted against M_0 in Fig. 10; apart from the expected decrease in the pressure difference as M_0 approaches unity, little consistency can be detected in this plot. It should be mentioned that no significance could be attached to shock position, except in so far as it is related to M_0 for each aerofoil configuration. However, one source of the scatter has become apparent from the results of tests on one aerofoil section in all the high-speed tunnel configurations of the Aerodynamics Division, National Physical Laboratory. It is found that the 'solidity' of the Mach-number freeze is greatly affected by the tunnel slotted-wall open/total area ratio used in the tests; moreover, the significance in this respect of a given open area is dependent on model incidence. To avoid confusion due to these tunnel-wall effects the analysis of the supersonic region is confined to results obtained from the N.P.L. 20 in. × 8 in. High-Speed Tunnel with 1/30th open/total area walls, and for zero-incidence tests only. These test conditions were chosen for detailed study because they are known to give smaller interference effects in the transonic range than the other tunnel configurations used (*see* Refs. 15 and 16). In Fig. 11 these pressure differences are plotted against the quantity $(M_0 - M^*)/(1 - M^*)$, where M^* is defined as the free-stream Mach number for which local

sonic speed is first reached at the aerofoil-surface crest, on the assumption of shock-free flow. This parameter is introduced to represent differences in aerofoil thickness and profile, and to assist in the comparison of results measured over different ranges of M_0. A useful mean curve can be drawn through the points of Fig. 11, and this is used to determine p_1/H_0 for a given free-stream Mach number from the corresponding sonic-range distribution. Fig. 12 shows this curve with pressure differences obtained under other test conditions.

In the following shock pressure-rise analysis, which is based on results obtained from all tunnel configurations, it is shown that p_1/H_0 is not an important parameter in the determination of shock position. In the application of the present scheme for the calculation of transonic pressure distributions a value of p_1/H_0 is essential in the estimation of the supersonic region, and the use of Fig. 11 is suggested to give consistent, and approximately tunnel-interference free, results.

To assist in the estimation of the supersonic pressure distribution upstream of a shock wave an analysis, similar to that described above for p_1/H_0, was carried out for the pressure differences at aerofoil surface crests. Again only results obtained in 1/30th open-area tunnel walls with zero model incidence were used. Fig. 13 shows these pressure differences, $(p_{CR} - p_{SR})/H_0$, plotted against $(M_0 - M^*)/(1 - M^*)$; it is seen that a useful mean curve can be drawn through the results. Pressure differences obtained from other tests are compared with this mean in Fig. 14.

2.2.2. *Shock pressure-rise.* A large number of measured shock pressure-rise ratios p_2/p_1 are shown plotted against p_1/H_0 in Fig. 15. No consistent trends in these results with respect to flow or geometric parameters is evident, and it is thought that much of the scatter is due to uncertainties in the analysis of measured pressure distributions. It is clear from the typical distributions shown in Figs. 6 to 9 that p_2/H_0 can usually only be obtained by graphical interpolation between pressure-hole positions, and values so obtained clearly cannot define detailed local pressure changes in the neighbourhood of a shock wave. Also the chordwise extent of shock-wave boundary-layer interaction probably differs from case to case. To overcome these difficulties in the interpretation of experimental results, the pressure immediately behind a shock is defined as that given by the Glauert compressibility rule applied at the same chordwise position to a corresponding measured shock-free flow. Values obtained in this way are denoted p_{2G}, and throughout this analysis were obtained from pressure distributions measured at $M_0 = 0{\cdot}70$. It is suggested in the Introduction that it is consistent to analyse measured distributions on this basis, using observed shock positions, provided that the pressure changes for some region downstream of the shock position are in accordance with those estimated by the Glauert rule. Only experimental results which satisfy this condition are considered. In fact, as no wake pressure-distribution measurements were available, only results which agree with those derived by the Glauert formulae at least at the trailing edge are used. The significance of these assumptions as regards the pressure distribution behind a shock wave on an aerofoil surface and the wake flow is discussed in Section 2.5.1.

In Fig. 16 the shock pressure-rise ratio p_{2G}/p_1 is shown plotted against p_1/H_0, the results being obtained from a number of observed shock positions on sixteen different aerofoil configurations. It is seen that a reasonable correlation is obtained, independent of aerofoil section or other flow characteristics. A mean curve is drawn through the points and the shock pressure-rise relation given by this is used in the prediction of transonic pressure distributions described in the following Section. It is interesting to note that this empirical relation is not greatly different from that obtained on the assumption that p_{2G}/H_0 has the constant value $0{\cdot}52$. This similarity explains the previously

mentioned insensitivity to p_1/H_0 of the comparison of values of p_{2G}/p_1. An assessment of the significance of the scatter of the values on Fig. 16 in terms of aerofoil shock position is given later. To assist in the later discussion of the result the mean curve of Fig. 16 is shown in Fig. 17, together with curves obtained with constant p_{2G}/H_0 and from the exact normal-shock equation.

2.3. *Application of the Empirical Scheme for the Prediction of Transonic Pressure Distributions.* In this Section it is shown how the results of the analysis of Section 2.2 can be used to predict transonic pressure distributions from a knowledge of the geometry of an aerofoil and its pressure distribution in wholly subsonic flow. The method is described by proceeding through the stages of a typical calculation.

The calculation of the upper-surface pressure distribution over a $9\frac{1}{2}$ per cent thick aerofoil at 2 deg incidence for free-stream Mach numbers of $0{\cdot}75$, $0{\cdot}80$ and $0{\cdot}82$ is set out in Tables 1 to 4, and is illustrated for $M_0 = 0{\cdot}80$ in Fig. 18. Table 1 gives the $M_0 = 1{\cdot}0$ (sonic-range) pressure distribution from crest to trailing edge as calculated by the theory of Ref. 2; this is also shown on Fig. 18. Table 2 lists the pressure distribution measured at $M_0 = 0{\cdot}70$ for the NACA 0009_5 at 2 deg incidence followed by the distributions calculated from this by the Glauert rule for $M_0 = 0{\cdot}75$, $0{\cdot}80$ and $0{\cdot}82$. The results for $M_0 = 0{\cdot}80$ are also shown on Fig. 18. The next stages in the calculation are based on the empirical relationships established in the preceding Sections of this paper. Table 3(a) shows the quantity $(M_0 - M^*)/(1 - M^*)$ tabulated against M_0; the corresponding values of $(p_1 - p_{SR})/H_0$ and $(p_{CR} - p_{SR})/H_0$ are then read off from the mean curves of Figs. 11 and 13. In Table 3(b) values of p_1/H_0 for each Mach number derived from Tables 1 and 3(a) are listed for the appropriate chordwise positions. It should be emphasised that, on the basis of the preceding analysis, the difference $(p_1 - p_{SR})/H_0$ has significance only at the relevant shock position. However, in the construction of a solution for a given M_0, it will be seen to be convenient to derive a locus of possible values of p_1/H_0 for the prescribed M_0 for a small chordwise region. The calculation can be limited to a few points from the knowledge that the shock pressure-rise relation leads to only small changes in p_{2G}/H_0 with changes in p_1/H_0. To return to Table 3(b), the shock pressure-rise ratio p_{2G}/p_1 corresponding to each value of p_1/H_0 is taken from Fig. 16, and p_{2G}/H_0 calculated. In this way a p_{2G}/H_0 locus for each free-stream Mach number is derived from the corresponding p_1/H_0 locus. The broken lines on Fig. 18 define these loci for $M_0 = 0{\cdot}80$. Now from the assumptions in the analysis leading to the empirical relationships the intersection of the p_{2G}/H_0 locus with the downstream distribution estimated by the Glauert rule for the appropriate free-stream Mach number defines the shock position for that Mach number; also at this position, x_S/c, the assumption in the analysis for p_1/H_0 holds, and hence p_1/H_0 is determined. There remains the calculation of the pressure distribution between the crest and shock position. The pressure at the crest for each free-stream Mach number is obtained from the values of $(p_{CR} - p_{SR})/H_0$ given in Table 3(a), and the sonic-range value. To estimate the pressure distribution from crest to shock position, that is, from p_{CR}/H_0 to p_1/H_0, it is sufficient to interpolate linearly with respect to chordwise position for the pressure differences from the sonic-range distribution. If $X = (x - x_{CR})/(x_S - x_{CR})$, then

$$(p - p_{SR})/H_0 = (p_{CR} - p_{SR})/H_0 + \{(p_1 - p_{SR})/H_0 - (p_{CR} - p_{SR})/H_0\}\, X\,.$$

In the example considered this calculation is trivial for $M_0 = 0{\cdot}75$ and is only set out for $M_0 = 0{\cdot}80$ and $0{\cdot}82$ in Table 4.

The estimated pressure distributions for $M_0 = 0{\cdot}75$, $0{\cdot}80$ and $0{\cdot}82$ are shown on Fig. 19 together with the corresponding measured values.

2.4. *Details of the Experimental Results Analysed.* The two-dimensional aerofoil pressure distributions analysed in this paper were all obtained in the high-speed wind tunnels of the Aerodynamics Division, N.P.L. The tests on the NPL 491 section are described in Ref. 17. Detailed results for the 4, 6 and 10 per cent RAE 104 sections and for the NACA 0009_5 with two modifications, the 6 per cent RAE 102, the 4 per cent biconvex and the 9 per cent thick cambered section, are as yet unpublished. Some comments on these tests are given below; the profiles of the above aerofoils are shown in Fig. 20.

All tests were made with boundary-layer transition fixed near the leading edge by a strip of carborundum powder. The basic and modified NACA 0009_5, the 4, 6 and 10 per cent RAE 104, and the 6 per cent RAE 102 sections were tested in the N.P.L. 20 in. × 8 in. High-Speed Wind Tunnel with slotted walls of open/total area ratio of 0·033. The 10 per cent RAE 104 profile has also been tested in this tunnel with 0·125 open walls and with solid walls. It is these tests which have shown the importance of test conditions in the correlation of measured aerofoil data. The NPL 491 and 4 per cent biconvex sections were tested in the N.P.L. 36 in. × 14 in. Wind Tunnel with slotted walls of 0·1 open/total area ratio.

The semi-empirical method of Ref. 2, which is used to calculate the sonic-range pressure distribution as part of the mixed-flow method of this paper was also based mainly on results obtained in the N.P.L. 20 in. × 8 in. Wind Tunnel.

2.5. *Discussion.* In this Section the significance of the analysis of Section 2.2 is considered in relation to the physical mechanism of transonic flows. The applicability of the method for calculating transonic pressure distributions is discussed, and the accuracy of the results obtained is assessed by comparison with the initial experimental data.

2.5.1. *Physical mechanism of mixed subsonic/supersonic flows.* Before discussing the significance of the empirical relations established in this paper the following convention will be adopted. It is noted in Part I that the pressure fall associated with the normal pressure-gradient reversal through a normal shock wave on an aerofoil surface is distributed over a limited chordwise region, and that this effect is probably influenced by the shock-wave boundary-layer interaction in a real flow. As it is not possible to calculate this pressure distribution reliably, it is convenient to suppose that the total pressure change can be represented as occurring at the shock position. This convention is illustrated below in Sketch A.

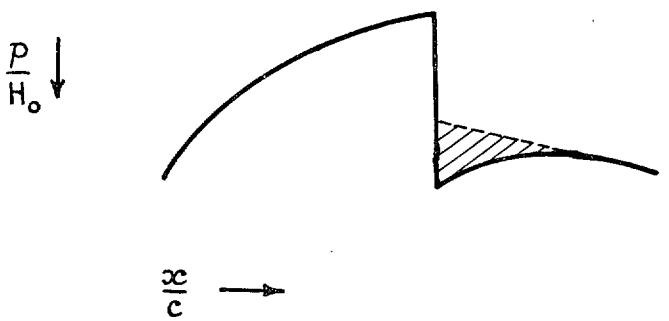

Sketch A

The full line represents the true pressure distribution and the hatched area the pressure changes due to the curvature singularity* following the shock. The assumption that this pressure distribution is concentrated at the shock position is equivalent to the replacement of the true distribution downstream of the shock by that shown by the broken line.

It is suggested that the empirical relations established are consistent with the attainment of the equivalent shock-free flow† downstream of a shock wave. The pressure distribution downstream of a shock given by the convention defined above would thus be that obtained on the assumption of shock-free flow. This hypothesis accounts for the finding that measured pressure distributions in the vicinity of the trailing edge of an aerofoil are related by a simple compressibility correction formula, even though shock waves are present in the flow upstream. Also the relation for the shock downstream pressure defined on the same basis (as p_{2G}/H_0) established in Section 2.2.2, suggests that the equivalent shock-free flow has some significance at this position. It is suggested that for a given shock upstream pressure (p_1/H_0) the difference between the value of p_2/H_0 given by the exact normal-shock equation and that estimated on the assumption of shock-free flow (p_{2G}/H_0) is the total effect of the pressure changes due to the curvature singularity at the shock position. The physical mechanism of the flow can then be deduced as follows: The pressure changes through a shock wave are to be thought of as including a full normal-shock pressure rise followed by a pressure fall dependent on the bounding-streamline curvature singularity. The shock position for a given free-stream Mach number is then determined by the necessity for the resultant shock downstream pressure to be continuous with the shock-free flow consistent with the prescribed free-stream conditions. This hypothesis implies that the replacement of an artificial, smoothly decelerating, supersonic flow by a real supersonic flow terminating in a shock wave does not significantly affect the subsonic flow downstream.

Attention is drawn to the measured pressure distributions shown in Figs. 21a and 21b. In Fig. 21a wholly subsonic flow results for the basic NACA 0009_5 section are compared with those at the same Mach number and incidence for two modified forms of this section. The modifications consist of different forms of drooped leading-edge extension (*see* Fig. 20) which give large changes from the basic pressure distribution forward of the crest of the surfaces, but are seen to have a negligible effect over the rear part of the sections. Fig. 21b shows a similar comparison between the subsonic-flow pressure distributions over a 14 per cent thick aerofoil with two leading-edge shapes (*see* Fig. 20); again, although there are large differences in the pressure distribution near the leading edge, there is no effect of the change in leading-edge shape on the rest of the pressure distribution. The significance of the change in the type of supersonic flow over the forward part of an aerofoil mentioned above is thus suggested as analogous to a change in aerofoil shape under conditions in which the flow type is unchanged, in that neither has a significant effect on the downstream flow. In either case it would seem necessary that the flow or geometry change has no more than a local effect on the boundary-layer development, particularly for flows with circulation.

The assumption that the pressure changes due to the boundary curvature singularity at a shock occur at the shock position is not essential to the above discussion. The chordwise distribution

---

* Whether these pressure changes are directly due to the singularity or to some other local flow behaviour is irrelevant to this discussion.

† The 'equivalent shock-free' flow is that obtained for the prescribed free-stream Mach number on the assumption of subsonic flow, although it will usually include a (unreal) region of supersonic flow; here it is taken as that given by the Glauert rule applied to a wholly subsonic flow.

associated with the singularity can be regarded as superimposed on the pressure distribution associated with the geometry of the surface.

Consideration of the wake flow can also go some way towards the explanation of the relation between real transonic flows and the corresponding shock-free flows. The coincidence of the pressure distribution from some distance downstream of a shock wave with that predicted for shock-free flow can be explained on the basis of the similarity of the pressure changes along the wake in the two flows.

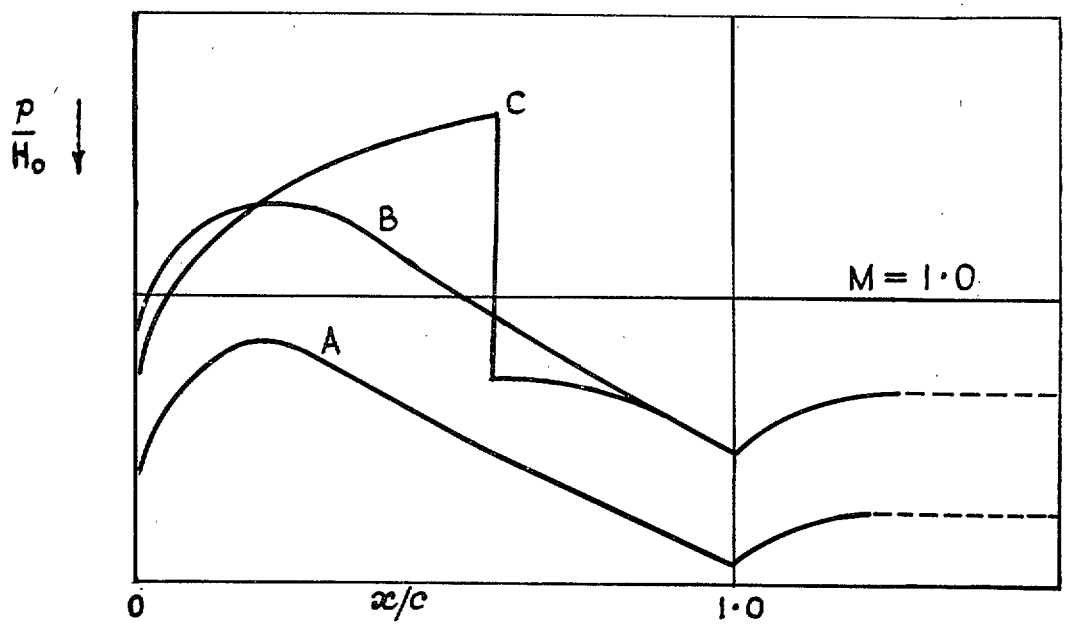

Sketch B

In Sketch B three pressure distributions are sketched. That denoted A represents the wholly subsonic flow at some free-stream Mach number M_A; pressure changes along the wake are shown and the broken line indicates the attainment of the free-stream conditions. Distribution B is that estimated for M_B from distribution A on the assumption of shock-free, subsonic-type, flow; distribution C corresponds to the real flow at M_B. It is supposed that the difference in flow between B and C does not significantly affect the boundary-layer parameters, which then will be similar to those associated with curve A. The wake characteristics associated with distribution C will therefore be the same as those associated with B, so that the pressure changes along the wake (*see* Ref. 1) in flow types B and C will be the same, and related to those associated with distribution A by simple compressibility considerations. It follows that the trailing-edge pressure of distributions C and A will also be so related. Moreover, since the stream-tube pattern must then be similar at the trailing edge, and the surface geometry ahead of the trailing edge is unaltered, the pressure distribution for some distance ahead of the trailing edge would be expected to be simply related. This wake flow mechanism cannot, however, be seen to lead to the significance of shock-free-type flow from immediately downstream of a transonic shock wave. Nevertheless, the satisfaction of the downstream boundary conditions *via* similar wake flows may account in some part for the correlation between

real and shock-free transonic flows, and between wholly subsonic flows with limited geometric modifications.

The hypothesis that the shock pressure-rise ratio p_{2G}/p_1 represents the overall pressure changes associated with a transonic shock wave would seem to be supported by the close agreement with the empirical curve for p_{2G}/p_1 of Emmons[6] theoretical results, as shown on Fig. 17. However, the strength of the boundary curvature singularity associated with a normal-shock wave is simply demonstrated by Emmons to be related to the shock upstream pressure and to the local surface curvature. Hence with each possible shock position the overall shock pressure changes should be related to both the local p_1/H_0 and surface curvature; the shock downstream pressure so obtained may be denoted $\bar{p}_2/H_0$. Then for a particular free-stream Mach number and aerofoil surface the locus of possible values of p_1/H_0 gives a unique $\bar{p}_2/H_0$ locus, as illustrated in Sketch C. In the sketch the equivalent shock-free pressure distribution over the rear part of the surface is also shown, and the previous

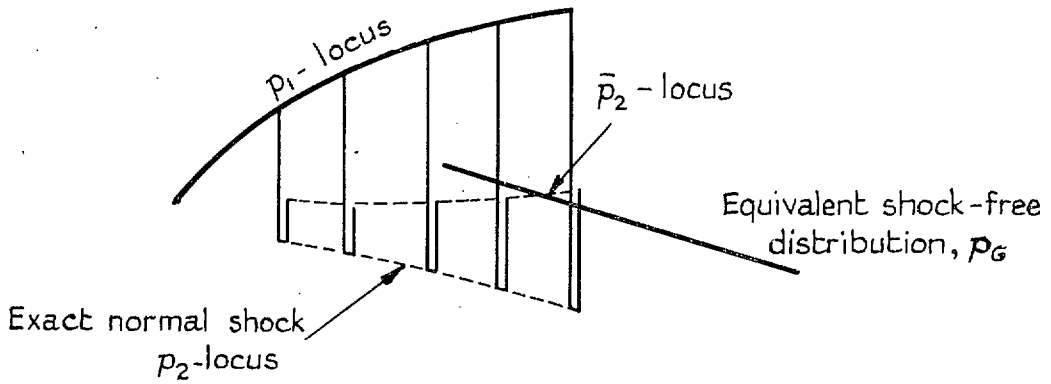

Sketch C

hypothesis is equivalent to assuming that the shock position is determined by the condition that $\bar{p}_2 = p_G$ $(= p_{2G})$. It is hence difficult to see why p_{2G}/p_1 appears as a function of p_1/H_0 only, and is not also dependent on the surface curvature at the shock position. For it is clearly possible to conceive cases with the same p_1, and hence (Fig. 16) the same p_{2G}, but with different surface curvatures at the shock positions.

In the hypothesis discussed earlier it is clearly not necessary to suppose that the pressure changes following a transonic shock wave on an aerofoil surface are due to an effective boundary curvature singularity, and indeed it appears that some other flow mechanism must be of equal or greater importance. The analysis of Gadd[13] (1957) suggests an alternative explanation of the non-attainment of the exact normal-shock pressure rise in observed flows. He suggests that as the boundary layer cannot withstand an abrupt pressure change it distorts to give a continuous simple-wave supersonic deceleration adjacent to the surface, which must clearly terminate at $M = 1{\cdot}0$. Downstream of this supersonic compression region the flow must satisfy the conditions imposed by (i) the geometry of surface, (ii) the pressure changes above the boundary layer, and (iii) the locally disturbed boundary layer. Condition (ii) is determined by the flow above the surface passing through a normal shock, and would be expected to lead to higher pressures than result directly from the compression to sonic conditions at the surface; this behaviour is illustrated in Fig. 22. This boundary-layer distortion mechanism avoids the necessity of a surface curvature singularity implicit in the assumption of a normal shock wave at the surface.

It is perhaps significant that the empirical shock pressure-rise relation gives values of p_{2G}/H_0 that correspond to near sonic flow downstream of shock waves. Thus the influence of conditions (ii) and (iii) above may be regarded as superimposed on the pressure distribution associated with the surface geometry, in the same way that the effects of a supposed curvature singularity have been treated. Shock-wave position would on this basis be determined from the necessity for the (sonic) pressure at the end of the supersonic compression region to be continuous with the 'geometry-dependent' pressure distribution, which has earlier been suggested as the equivalent shock-free subsonic-type distribution. Sketch D, which is analogous to Sketch A for the curvature singularity argument, illustrates this argument.

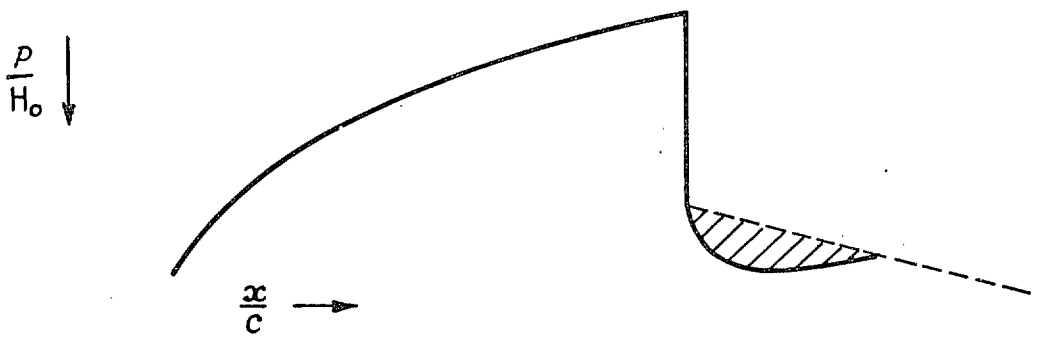

Sketch D

The full line represents an observed pressure distribution and the broken line the corresponding shock-free (geometry-dependent) distribution. The hatched area represents the pressure changes due to a high-pressure region behind the shock wave above the surface, and to other local effects at the shock position.

The preceding discussions of the physical mechanism of transonic flows clearly do not in either case fully explain the large discrepancies between measured shock-wave pressure changes and those given by exact shock-wave theory. Nevertheless, it is thought that the empirical shock pressure-rise relation gives useful results in conjunction with the rest of the empirical scheme for the prediction of transonic pressure distributions, and may also be valuable if suitably introduced into theoretical methods. However, the problem of shock waves on aerofoil surfaces will be further studied by experimental and theoretical methods. Flow studies of the type shown in Fig. 22 will form an important part of this research; it is interesting that these results suggest that the Gadd-type flow pattern is realised very near the surface, but that above the surface the pressure changes along streamlines are more in accordance with the mechanism suggested by Emmons.

2.5.2. *Applicability of empirical scheme.* In the analysis leading to the empirical relationships described in Section 2.2 only selected experimental results are used. Measured pressure distributions which appear to be incompatible with the physical basis of the analysis are excluded. Firstly, only results for which the conception of a Mach-number freeze is approximately valid have been used, so that pressure distributions which include leading-edge suction peaks are not included in the analysis. Such flows are closely related to aerofoil leading-edge geometry, and cannot be simply related to the sonic-range distribution by a function of free-stream Mach number only. Also, in the

analysis of supersonic regions empirical relations are derived from results obtained under one set of wind-tunnel conditions. This restriction was necessary to avoid the complicated and not fully understood effects of slotted-wall tunnel interference. The second major restriction follows from the discussion in Section 2.1 on the validity of using observed shock-wave positions in the analysis for the shock pressure-rise ratio. It is shown to be sufficient for the pressure recovery from some distance downstream of an observed shock position to be coincident with the assumed equivalent shock-free pressure distribution. In many cases this condition may only be satisfied in the wake flow, but as no wake pressure distributions were available the present analysis is restricted to results for which the condition appears to be satisfied at the trailing edge.

It is appropriate here to comment on the use of the Glauert compressibility rule for the calculation of shock-free transonic flows. The analysis of Ref. 14 suggests that this is the most useful of the well-known compressibility formulae for the estimation of pressure distributions in the trailing-edge region. For this reason, and because of its simplicity, the Glauert rule is used to estimate equivalent shock-free flows at other chordwise positions of interest. In all cases the basic, wholly subsonic, distribution is taken as that measured at $M_0 = 0{\cdot}70$. In some applications of the scheme developed here it might be convenient to use a theoretical subsonic pressure distribution as a starting point, and it is thought that results useful for comparative purpose would be obtained (*see* Fig. 18). However, as it is known that boundary-layer effects can significantly modify aerofoil pressure distributions, particularly for flows with circulation, it is preferable to use a measured subsonic distribution in the application of the scheme. It then follows from the nature of the scheme that major viscous effects are included throughout.

The analysis has also been limited to pressure distributions between the crest and trailing edge of aerofoil surfaces, primarily because it is only possible to estimate the sonic-range distribution for round-nosed aerofoils at incidence over this region. Also, no separate consideration of the lower surface of an aerofoil at incidence is included. In cases when the flow is of mixed subsonic/supersonic type the present analysis is relevant; if the lower-surface flow is wholly subsonic, the pressure distribution can again be estimated approximately by the Glauert rule.

To illustrate the accuracy of the method for estimating transonic pressure distributions Figs. 23 to 40 show comparisons between distributions calculated by the method and those used in its derivation. Some comparisons for results not used in the analysis are also shown. These measured distributions were excluded because they did not satisfy the 'shock-free flow at trailing edge' condition; such comparisons are distinguished by an asterisk. In nearly all cases good agreement for shock position is obtained, and this is further illustrated by direct comparison in Fig. 41. The large error in the calculated shock position for the 6 per cent RAE 104 at 2 deg incidence and $M_0 = 0{\cdot}85$ (denoted $\prec$ in Fig. 41) is probably associated with the very small chordwise variation of the shock-free flow pressure distribution in the region $0{\cdot}2 < x/c < 0{\cdot}6$ in this example, for a small error in the estimated values of p_{2G}/H_0 can then lead to a large error in shock position. The discrepancies between theory and experiment for the supersonic parts of the pressure distributions can mainly be attributed to the varied test conditions of the experimental results. It is interesting to note that errors in this part of the calculation do not necessarily lead to large errors in shock position, a feature of the method that is emphasised in Fig. 40, where results are compared for a high aerofoil incidence case with leading-edge suction peaks in the measured distributions. Differences between the calculated and measured distributions downstream of the shock waves are considered in detail in the previous Section.

It is encouraging that the method appears to give a good estimate of shock position even in those cases for which the estimated pressure distribution is less satisfactory. Shock position is probably the most important parameter in the assessment of high-speed aerofoil sections as it is closely related to the onset of the transonic drag-rise.

NOTATION

c		Aerofoil chord
H_0		Free-stream stagnation pressure
M, M_0		Local and free-stream Mach number, respectively
M^*		Crest critical Mach number
p		Local static pressure
x		Ordinate in free-stream direction, origin at aerofoil leading edge
y		Distance normal to aerofoil surface
X	$\equiv$	$(x - x_{CR})/(x_S - x_{CR})$
α		aerofoil incidence

Suffices

1, 2	Values immediately upstream and downstream of a shock wave, respectively
SR	Equivalent sonic-range value
CR	Crest value
S	Shock-wave value
	Value calculated by Glauert compressibility rule.

Application of Method

Calculations for NACA 0009_5, $\alpha = 2$ deg, $M_0 = 0{\cdot}75$, $0{\cdot}80$ and $0{\cdot}82$

TABLE 1

Sonic-range pressure distribution.
Calculated by the method of Ref. 6

	(Crest)								
x/c	0·22	0·30	0·40	0·50	0·60	0·70	0·80	0·90	1·00
p/H_0	0·383	0·364	0·345	0·334	0·332	0·330	0·330	0·337	0·342

TABLE 2

Subsonic (downstream of shock) part of pressure distribution.
Calculated from measured distribution for $M_0 = 0{\cdot}70$ by the Glauert compressibility correction formula

M_0	0·70	0·75	0·80	0·82
x/c	p/H_0	p/H_0	p/H_0	p/H_0
0·22	0·565	0·506		
0·30	0·588	0·530		
0·40	0·618	0·568	0·508	
0·50	0·645	0·600	0·550	0·527
0·60	0·667	0·625	0·580	0·561
0·70	0·668	0·650	0·610	0·594
0·80	0·708	0·675	0·639	0·625
0·90	0·730	0·699	0·669	0·657
1·00	0·756	0·730	0·705	0·695

TABLE 3

Estimation of Shock Position

(For the NACA 0009_5, $\alpha = 2$ deg, $M^* = 0{\cdot}730$)

(*a*) *Use of Figs.* 11 *and* 13

M_0	$M_0 - M^*$	$(M_0 - M^*)/(1 - M^*)$	$(p_1 - p_{SR})/H_0$	$(p_{CR} - p_{SR})/H_0$	p_{CR}/H_0
0·75	0·02	0·074	0·075	0·054	0·437
0·80	0·07	0·269	0·037	0·023	0·406
0·82	0·09	0·334	0·029	0·017	0·400

(*b*) *Calculation of* p_1/H_0 *and* p_{2G}/H_0 *loci*

x/c	$M_0 = 0{\cdot}75$			$M_0 = 0{\cdot}80$			$M_0 = 0{\cdot}82$		
	p_1/H_0	p_{2G}/p_1	p_{2G}/H_0	p_1/H_0	p_{2G}/p_1	p_{2G}/H_0	p_1/H_0	p_{2G}/p_1	p_{2G}/H_0
0·22	0·458	1·115	0·511						
0·30	0·439	1·183	0·519						
0·40				0·382	1·387	0·530			
0·50				0·371	1·427	0·530	0·363	1·455	0·529
0·60							0·361	1·462	0·528

TABLE 4

Calculation of supersonic pressures between crest and shock

$M_0 = 0{\cdot}80$

x/c	X	$(p - p_{SR})/H_0$	p/H_0
0·22	0	0·023	0·406
0·30	0·34	0·028	0·392
0·40	0·77	0·034	0·379
0·455	1·00	0·037	0·375

$M_0 = 0{\cdot}82$

x/c	X	$(p - p_{SR})/H_0$	p/H_0
0·22	0	0·017	0·400
0·30	0·28	0·020	0·384
0·40	0·63	0·025	0·370
0·50	0·98	0·029	0·363
0·505	1·00	0·029	0·362

PART III

ANALYSIS OF THEORETICAL SOLUTIONS

3.1. *Introduction.* To supplement the empirical analysis described in Part II of the present paper some calculations of transonic flows based on the theory of Spreiter and Alksne[3] (1955) have been made. In Part I it is suggested that this theory, which leads to an iterative solution of an integral form of the transonic flow equations, is the most advanced theoretical method available. It is shown here that results obtained by the method, although exhibiting some of the important features of transonic flow, do not compare well with experiment. This failure of the method is discussed, and it is shown how the empirical relations established in Part II can be combined with part of the theoretical solutions to give results in close agreement with experiment. It is suggested that these modifications could be directly incorporated into the analysis and thereby included in the iterative method of solution.

The derivation of the theory is given in Ref. 3 with additional results in Ref. 19. The general form of the equation solved for the local (reduced) perturbation velocity is given below:

$$\begin{aligned}\bar{u} = \bar{u}_L + \frac{\bar{u}^2}{2} - \frac{1}{2\pi}\iint_R \left(\frac{\bar{u}^2}{2}\frac{\partial}{\partial\bar{\xi}^2}\ln\frac{1}{r}\right)d\bar{\xi}\,d\bar{\zeta} + \\ + \frac{1}{2\pi}\int_S \left\{\left[\ln\frac{1}{r}\frac{\partial}{\partial\bar{\xi}}\left(\bar{u} - \frac{\bar{u}^2}{2}\right) - \left(\bar{u} - \frac{\bar{u}^2}{2}\right)\frac{\partial}{\partial\bar{\xi}}\ln\frac{1}{r}\right]_a - \right. \\ \left. - \left[\ln\frac{1}{r}\frac{\partial}{\partial\bar{\xi}}\left(\bar{u} - \frac{\bar{u}^2}{2}\right) = \left(\bar{u} - \frac{\bar{u}^2}{2}\right)\frac{\partial}{\partial\bar{\xi}}\ln\frac{1}{r}\right]_b + \right. \\ \left. + \left[\left(\ln\frac{1}{r}\frac{\partial\bar{u}}{\partial\bar{\xi}} - \bar{u}\frac{\partial}{\partial\bar{\xi}}\ln\frac{1}{r}\right)_a - \left(\ln\frac{1}{r}\frac{\partial\bar{u}}{\partial\bar{\xi}} - \bar{u}\frac{\partial}{\partial\bar{\xi}}\ln\frac{1}{r}\right)_b\right] \times \left[\frac{\cos(n,\,\bar{\zeta})}{\cos(n,\,\bar{\xi})}\right]_b\right\}d\bar{\zeta}\,. \qquad (4)\end{aligned}$$

The symbols are the same as those used in Ref. 3 and are defined in Section 3.6 of the present paper. The term $\bar{u}_L$ is the corresponding velocity perturbation for subsonic flow as defined by linearized theory. The first integral is taken over the whole flow field, R, and the second round the surface of the shock wave, S. However, this term is shown to be identically zero on the assumption of a normal shock wave with flow parallel to the x-axis. The integral over R is reduced to a single integral along $\bar{z} = 0$ by the following assumption for velocity variations normal to the $\bar{x}$-axis:

$$\bar{u}(\bar{x},\,\bar{z}) = \bar{u}_w(\bar{x},\,0)/(1 + \bar{z}f(\bar{x}))^2\,, \qquad (5)$$

where $f(\bar{x})$ is chosen to satisfy the irrotationality condition at $\bar{z} = 0$. It is found that

$$1/f(\bar{x}) = -\,2\bar{u}_w/(\partial^2\bar{Z}/\partial\bar{x}^2)\,.$$

The function $\bar{Z}$ is simply derived from the equation of the aerofoil surface, so that $f(\bar{x})$ is approximately proportional to surface curvature, and is therefore infinite upstream and downstream of the aerofoil. Equation (1) is thus reduced to the following form for the velocity on the surface

$$\bar{u}_w = \bar{u}_{L\,w} + \frac{\bar{u}_w^{\,2}}{2} - \int_0^c \frac{\bar{u}_w^{\,2}}{2b}E(f\overline{\bar{\xi} - \bar{x}})\,d\bar{\xi}\,. \qquad (6)$$

E is a known function of $f(\bar{\xi} - \bar{x})$. An iterative scheme is used to derive $\bar{u}_w$ for given initial conditions.

The presence of the term $\bar{u}_{L\,w}$ follows from the analysis, and the method does not consist explicitly of the derivation of second-order effects on the linearized solution. However, the form of this term does follow the assumption of only small perturbations about free-stream velocity, and also limits the sensible application of the method to aerofoils with finite leading-edge gradient. More accurate methods for the estimation of incompressible-flow velocity distributions exist, and if the contribution of the term $\bar{u}_{L\,w}$ in equation (6) is replaced by values derived from such a solution, not only might more accurate results be obtained but also the application of the method to round-nosed aerofoils presents no further difficulties. In the solutions calculated for this paper the term $\bar{u}_{L\,w}$ was replaced by corresponding values derived from Woods's[20] (1950) Polygon method for incompressible flow. This method is shown to give accurate solutions for zero-circulation flows in Ref. 21.

The theory of Ref. 3 postulates inviscid flow, so to examine its usefulness by comparison with experiment it is clearly necessary to reduce viscous effects in the experiments to a minimum. Viscous effects assume great importance in the study of flows which include shock waves as it is well known that shock-wave boundary-layer interaction can considerably affect the development of transonic flows, particularly if separation of the boundary layer is induced. The theory has therefore been applied to two profiles for which measured pressure distributions are available which do not include large effects of shock-wave boundary-layer interaction. The NPL 491 section was designed to give relatively low supersonic speeds over its surface at low incidence for all transonic free-stream speeds, so that shock waves on the surface would not induce separation. The Kaplan 10 per cent thick bi-cusped-profile model has a porous surface so that the boundary-layer thickness can be greatly reduced, and separation eliminated, by suction. Experimental results have also been obtained for a 4 per cent thick biconvex section for comparison with the solutions given in Ref. 3.

As a further check on the transonic theory sub-critical pressure distributions for these profiles have also been calculated by the Polygon method. From the excellent agreement with the method of Ref. 3 obtained it appears that the approximations introduced into the later method to permit mixed-flow solutions with shock waves do not lead to errors in the calculation of wholly subsonic flows.

In Section 3.2 the comparisons between theory and experiment for transonic flow are discussed with reference to the simplifying assumptions introduced into the mathematical analysis. It is demonstrated that the large discrepancies between theory and experiment can be associated with the assumption of a full normal-shock pressure rise in the theory. Combination of the theoretical solutions with the results of the empirical analysis of Part II is shown to improve greatly the correlation between the calculated and measured pressure distributions. The use of these results follows from the discussion of the physical mechanism of transonic flows given in Part II, and the success obtained is evidence in favour of the suggested flow mechanism.

3.2. *Comparisons Between Theory and Experiment.* Before considering in detail the comparisons between calculated and measured pressure distributions the following points must be noted. Firstly, the theoretical solutions are obtained at ten chordwise positions only, equally spaced from $0{\cdot}05c$ to $0{\cdot}95c$. Secondly, the assumption of a particular form for the velocity variation normal to the chord-line (*see* equation (5)) may not be valid for supersonic flow at positions of zero surface curvature.

Because of this no detailed consideration is given to a solution for the NPL 491 profile with trailing-edge shock position; in the other transonic solutions for that profile the supersonic flow is confined to regions of non-zero curvature. Similarly, in the transonic solution for the bi-cusped profile the points of inflexion of the profile are in regions of subsonic flow.

Figs. 42a, 42b and 42c show the calculated and measured pressure distributions for the NPL 491, biconvex and bi-cusped profiles respectively. Where sufficient data are available experimental results are given for the free-stream Mach numbers of the calculated pressure distributions, and for the Mach numbers for which the observed shock positions coincide with those predicted by the theory.

A consistent feature of the comparisons is the finding that the observed shock position for a given free-stream Mach number is upstream of that predicted by the theory. The calculated pressure distributions upstream of the observed shock positions and downstream of the theoretical shock positions are, however, in good agreement with experiment. This is not so if the comparisons are made for the same shock positions, and the comparisons cannot be usefully considered from this aspect.

It is suggested that the large discrepancies in shock position for a given free-stream Mach number can be attributed to the assumption in the analysis that the pressure rise in the vicinity of the shock is that given by the normal-shock equation, as this is incompatible with the assumed pressure variation normal to the chord-line. The mechanism of normal-shock-wave bounding-streamline interaction is fully discussed in Part I. It is shown that the presence of a normal shock on a curved surface necessarily leads to a reversal of the pressure gradient normal to the surface, and hence to a discontinuity in bounding-streamline curvature and a consequent pressure fall. Now in the theory no solution is obtained at the shock-wave position itself, and following the assumption of a normal shock the shock integral vanishes identically; equation (5) is also clearly incompatible with a reversal in the normal pressure gradient. Hence the analysis permits no representation of local flow changes at the shock position, and by prescribing a boundary condition which is more relevant to shock-free flow tends to give pressure changes from immediately behind the assumed shock position in accordance with the equivalent shock-free flow. It is shown in Part I that these assumptions will inevitably lead to shock positions downstream of those observed in tunnel tests at the same free-stream Mach numbers.

The empirical shock pressure-rise relation established in Part II is shown there to be defined in such a way as to take into account the overall local pressure changes due to shock-wave bounding-streamline interaction. This relation would appear more appropriate to the theory of Ref. 3 than the classical normal-shock relation, and is not necessarily incompatible with the assumption implied by equation (5). It is suggested in Section 3.3 that this relation could be incorporated into the method of solution of Ref. 3; however, it is possible to derive the corresponding solutions by modifying those already obtained.

Fig. 43 shows the pressure distributions downstream of the assumed shock positions as calculated by Spreiter and Alksne's theory compared with those estimated for the same values of M_0 by the Glauert compressibility formula from a wholly subsonic-flow solution. It is seen that other than immediately downstream of the theoretical shock positions good agreement is obtained; this is in accordance with the suggestions of Part II. It appears that for more forward shock positions the theory would give pressure distributions downstream of shocks similar to those calculated by the Glauert rule, and hence that they may be simply estimated.

The physical mechanism of the supersonic-flow development at a prescribed free-stream Mach number suggests that the associated surface-pressure distribution is little affected by shock position, and the analysis of Section 2.2.1 confirms this view. The supersonic distribution calculated by the method of Ref. 3 may thus be taken as a locus of possible values of the shock upstream pressure, p_1, for the prescribed free-stream Mach number. Then in a similar way to the construction of pressure distributions described in Part II, the empirical shock pressure-rise relation defines a p_{2a} locus whose intersection with the appropriate shock-free flow distribution defines the shock position. This procedure has been applied to the theoretical results shown in Fig. 42, and the resultant pressure distributions are shown in Fig. 44 together with the appropriate experimental results. It is seen that a great improvement over the unmodified theoretical results is obtained. To illustrate further the comparison of both the direct and modified theory with experiment the shock positions are shown in Fig. 45 as a function of free-stream Mach number.

The theory of Spreiter and Alksne is valid only for the flow about a symmetrical aerofoil at zero incidence, but for this case when modified as above it has the advantage over the empirical method developed in Part II of giving the whole of the chordwise pressure distribution. Part II, while not restricted to zero-circulation flows, considers the pressure distribution downstream of an aerofoil surface crest only.

3.3. *Possible Introduction of Empirical Shock Relation into Theoretical Method.* In Section 3.1 equation (4) gives the form of the transonic flow equation solved by Spreiter and Alksne after two further approximations to the real flow*; the assumption of the normal-shock equation and of a certain form of velocity variation normal to the surface. The authors of Ref. 3 note that these two assumptions are mutually incompatible except at the surface, but suggest that this is only of importance for relatively strong shock waves. However, wind-tunnel results suggest that the local flow behaviour in the neighbourhood of a shock wave is of great importance, even though the shock strength be small. It has been suggested earlier that these effects are included in the empirical shock relation established in Part II, and shown that when this is introduced into the theoretical solutions by graphical methods more realistic results are obtained. In this Section the inclusion of the empirical relation directly into the numerical method of solution is briefly considered.

In Ref. 3 it is shown that the normal-shock equation (in normalised form and for small perturbations) is equivalent to stating that

$$\bar{u}_a - \frac{\bar{u}_a^2}{2} = \bar{u}_b - \frac{\bar{u}_b^2}{2},$$

where a and b denote values immediately upstream and downstream of a shock, respectively. Also, from the equation of continuity,

$$\frac{\partial}{\partial \bar{\xi}}\left(\bar{u}_a - \frac{\bar{u}_a^2}{2}\right) = \frac{\partial}{\partial \bar{\xi}}\left(\bar{u}_b - \frac{\bar{u}_b^2}{2}\right) = 0.$$

* Other approximations are introduced to facilitate the numerical solution of the equation by an iterative process.

It is clear that these two relations, and the assumption that the shock is normal to the streamlines, eliminate the shock integral of equation (4). If a normal-shock wave, but not the classical shock pressure-rise relation, is assumed, the following shock integral remains:

$$-\frac{1}{2\pi}\int_S \left\{\left[\left(\bar{u}-\frac{\bar{u}^2}{2}\right)\frac{\partial}{\partial\bar{\xi}}\ln\frac{1}{r}\right]_a-\left[\left(\bar{u}-\frac{\bar{u}^2}{2}\right)\frac{\partial}{\partial\bar{\xi}}\ln\frac{1}{r}\right]_b\right\}d\bar{\zeta}\,. \tag{7}$$

The inclusion of this integral in numerical solutions requires firstly a relation for $\bar{u}_b$ in terms of $\bar{u}_a$, and secondly some means of determining the limits of integration. For a normal shock wave with flow parallel to the x axis the contour S is a straight line normal to the $\bar{x}$ axis and the limits of integration are $\bar{\zeta}=0$ and $\bar{\zeta}=\bar{z}_s$, where $\bar{z}_s$ is the height of the shock wave. It appears sensible on physical grounds to choose $\bar{z}_s$ as the value of $\bar{z}$ which gives local sonic conditions ahead of the shock wave on the basis of equation (5). The empirical shock relation established in Part II of the present paper is derived from surface-pressure distributions and would not be expected to be valid above the surface of an aerofoil. Indeed the static-pressure traverses through a shock wave shown in Fig. 22 and those obtained by Ackeret, Feldman and Rott[22] (1946) indicate that the pressure rise through a shock some distance above the surface is more in accordance with that given by the classical normal shock equation. It is suggested therefore that the shock integral be evaluated as follows:

(i) $\bar{u}_{w\,a}$ is determined from a solution in which the shock integral is neglected.

(ii) $\bar{u}_{w\,b}$ is calculated from $\bar{u}_{w\,a}$ and the empirical shock relation.

(iii) $\bar{u}_a$ is calculated from $\bar{u}_{w\,a}$ and equation (5).

(iv) The exact normal shock equation (transonic approximation) can be used to calculate values of $\bar{u}_b$ from $\bar{u}_a$; let values so obtained be denoted $\bar{u}_b'$.

(v) Values of $\bar{u}_b$ may also be calculated from $\bar{u}_{w\,b}$ by equation (5), these will be denoted $\bar{u}_b''$. Then if $\bar{u}_b'=\bar{u}_b''$ at $\bar{\zeta}=\bar{z}_s'$, it is suggested that for the evaluation of the shock integral $\bar{u}_b$ be taken as $\bar{u}_b''$ for $0\leqslant\bar{\zeta}\leqslant\bar{z}_s'$ and as $\bar{u}_b'$ for $\bar{z}_s'\leqslant\bar{\zeta}\leqslant\bar{z}_s$. This approach should give a reasonable approximation to the physics of the flow in the neighbourhood of a shock wave, whilst retaining the assumptions implied by the use of equation (5) to simplify the original integral equation derived by Spreiter and Alksne. The shock integral, equation (7), now reduces to

$$-\frac{1}{2\pi}\int_0^{\bar{z}_s'}\left\{\left(\left[\bar{u}-\frac{\bar{u}^2}{2}\right]\frac{\partial}{\partial\bar{\xi}}\ln\frac{1}{r}\right)_a-\left(\left[\bar{u}-\frac{\bar{u}^2}{2}\right]\frac{\partial}{\partial\bar{\xi}}\ln\frac{1}{r}\right)_b\right\}d\bar{\zeta}\,.$$

3.4. *Concluding Remarks.* In Part I of the present paper it is suggested that the transonic theory of Spreiter and Alksne is the most advanced analytical method for the prediction of mixed subsonic/supersonic pressure distributions. In this paper it is shown that the application of the theory can be simply modified to extend its applicability to round-nosed aerofoils. Calculated solutions are, however, found to differ greatly from those obtained by experiment, and it is suggested that this can be attributed to misrepresentation of the shock waves and associated flow changes. Nevertheless, by the introduction of the results of the analysis of Part II, and application of the suggested flow mechanism following the analysis, useful results are obtained.

3.5. *Acknowledgements.* The authors are indebted to Mr. W. E. A. Acum, of the Aerodynamics Division, N.P.L., for his supervision of the calculations by the method of Ref. 3 reported here.

NOTATION

c		Aerofoil chord
f		Function of $\bar{x}$; related to boundary condition on wing
H_0		Free-stream stagnation pressure
k		Coefficient of non-linear term in differential equation for velocity potential
M_0		Free-stream Mach number
n		Normal to shock surface
p		Static pressure
r	$\equiv$	$\{(\bar{x} - \bar{\xi})^2 + (\bar{z} - \bar{\zeta})^2\}^{1/2}$
u		Perturbation velocity component parallel to x-axis
$\bar{u}$	$\equiv$	ku/β^2
x, z		Cartesian ordinates, x-axis in direction of free stream
$\bar{x}$	$\equiv$	x
$\bar{z}$	$\equiv$	βz
α		Aerofoil incidence
β	$\equiv$	$(1 - M_0^2)^{1/2}$
$\bar{\xi}$, $\bar{\zeta}$		Variables of integration corresponding to $\bar{x}$, $\bar{z}$
τ	$\equiv$	$M_0^2(\gamma + 1)/(1 - M_0^2)^{3/2}$

Suffices

a, b : 1, 2	Values immediately upstream and downstream of a shock wave respectively
G	Calculated by Glauert rule from a corresponding subcritical flow
L	Values given by linear theory
s	Value at shock position
w	Values at wing surface

M_* ?? ballon 11

REFERENCES

No.	Author	Title, etc.
1	H. H. Pearcey	Some effects of shock-induced separation of turbulent boundary layers on transonic flow past aerofoils. Paper No. 9 presented at the Symposium on Boundary-Layer Effects in Aerodynamics, at the National Physical Laboratory, 31st March/2nd April, 1955. R. & M. 3108. June, 1955.
2	C. S. Sinnott	On the flow of a sonic stream past an aerofoil surface leading to a semi-empirical method for the prediction of sonic-range pressure distributions. *J.Ae.Sp.Sci.* November, 1959.
3	J. R. Spreiter and A. Alksne ..	Theoretical prediction of pressure distributions on non-lifting airfoils at high subsonic speeds. N.A.C.A. Report 1217. 1955.
4	C. S. Sinnott	A method of computing subsonic and transonic plane flows. C.P. 173. September, 1953.
5	H. W. Emmons	Flow of a compressible fluid past a symmetrical airfoil in a wind tunnel and in free air. N.A.C.A. Tech. Note 1746. November, 1948.
6	H. W. Emmons	The theoretical flow of a frictionless, adiabatic, perfect gas inside of a two-dimensional hyperbolic nozzle. N.A.C.A. Tech. Note 1003. May, 1946.
7	D. Meksyn	Integration of the equations of transonic flow in two dimensions. Communicated by A. Page. *Proc. Roy. Soc.* A. Vol. 220. pp. 239 to 254. 1953. A.R.C. 15,412. November, 1952.
8	C. S. Sinnott	An experimental investigation of Meksyn's transonic inviscid-flow theory. C.P. 302. November, 1955.
9	Isao Imai	Approximate methods in compressible fluid dynamics. Parts I and II. University of Maryland, Institute for Fluid Dynamics and Applied Maths. Tech. Note BN–95. March, 1957.
10	K. Oswatitsch	Die Geschwindigkeitsverteilung bei lokalen Uberschallgebieten an flachen Profilen. *Z.A.M.M.* Bd. 30. No. 1/2. January/February, 1950. Die Geschwindigkeitsverteilung an symmetrischen Profilen beim Auftreten lokaler Uberschallgebiete. *Acta Physica Austriaca.* Bd. 4. No. 2/3. December, 1950.
11	T. R. Gullstrand	The flow over symmetrical aerofoils without incidence in the lower transonic range. K.T.H. Aero. Tech. Note 20. 1952.
12	W. R. Sears (editor)	*General Theory of High-Speed Aerodynamics. Section F.* Oxford University Press.
13	G. E. Gadd	The interaction between a weak normal shock wave and a turbulent boundary layer. C.P. 424. June, 1957.

REFERENCES—*continued*

No.	*Author*	*Title, etc.*
14	J. Osborne and C. S. Sinnott . .	The use of simple compressibility formulae for transonic flow. A.R.C. 21,860. April, 1960.
15	D. W. Holder, R. J. North and A. Chinneck	Experiments with slotted and perforated walls in a two-dimensional high-speed tunnel. R. & M. 2955. November, 1951.
16	H. H. Pearcey, C. S. Sinnott and J. Osborne	Some effects of wind-tunnel interference observed in tests on two-dimensional aerofoils at high subsonic and transonic speeds. N.P.L. Aero. Note 373. February, 1959.
17	D. W. Holder and R. F. Cash . .	Experiments with a two-dimensional aerofoil designed to be free from turbulent boundary-layer separation at small angles of incidence for all Mach numbers. R. & M. 3100. August, 1957.
18	C. S. Sinnott	Estimation of the transonic characteristics of aerofoils. N.P.L. Aero. Note 385. July, 1959.
19	J. R. Spreiter, A. Alksne and B. J. Hyett	Theoretical pressure distributions for several related non-lifting airfoils at high subsonic speeds. N.A.C.A. Tech. Note 4148. 1958.
20	L. C. Woods	The two-dimensional subsonic flow of an inviscid fluid about an aerofoil of arbitrary shape. Parts I to IV. R. & M. 2811. November, 1950.
21	C. S. Sinnott	Calculated velocity distributions and force derivatives for a series of high-speed aerofoils. R. & M. 3045. December, 1955.
22	J. Ackeret, F. Feldmann and N. Rott	Investigations on compression shocks and boundary layers in fast moving gases. Institute for Aerodynamics, E.T.H. Zurich. No. 10. 1946. A.R.C. 10,044. September, 1946.

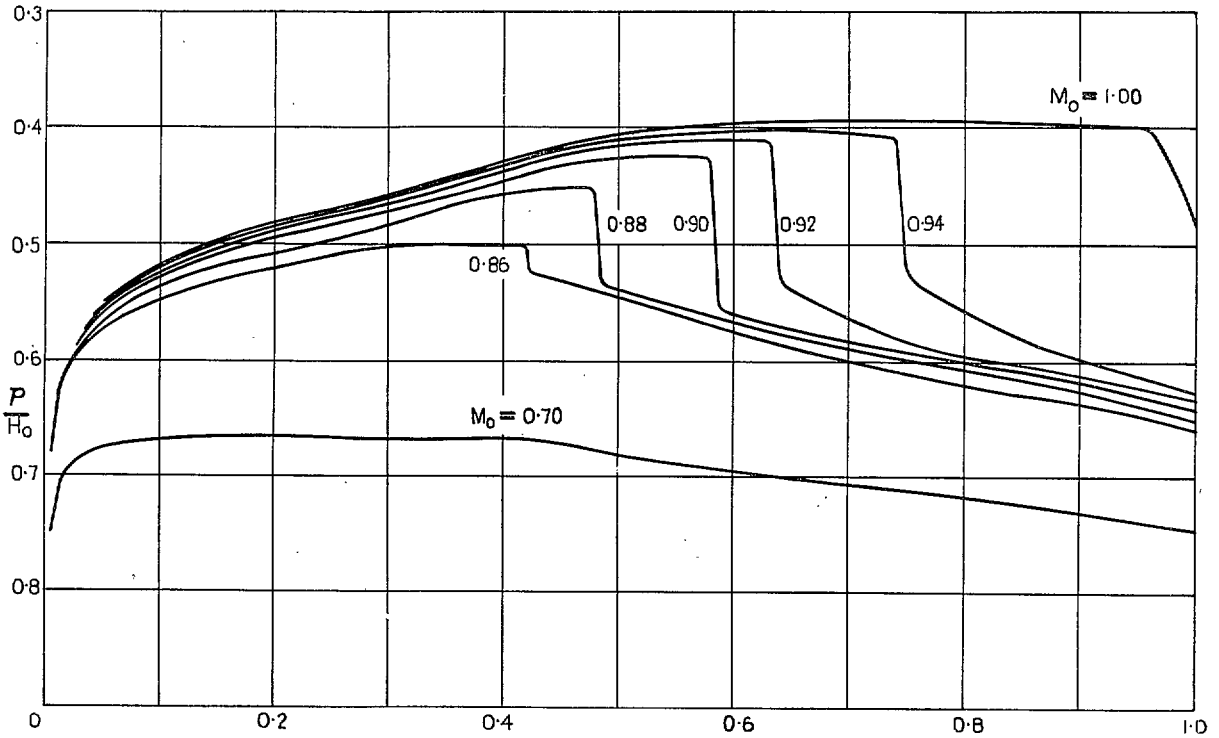

FIG. 1. Typical family of transonic pressure distributions.

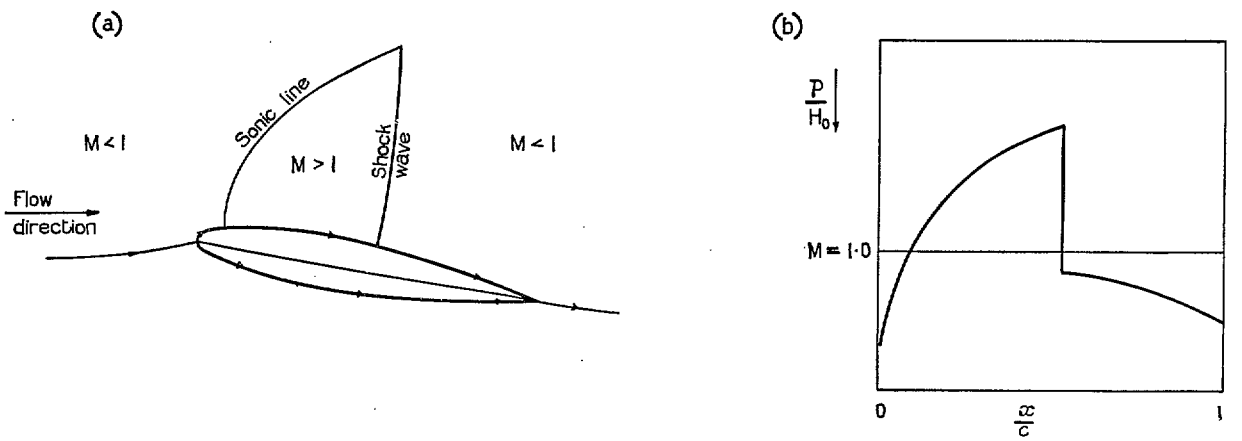

FIGS. 2a and 2b. Transonic flow pattern and pressure distribution.

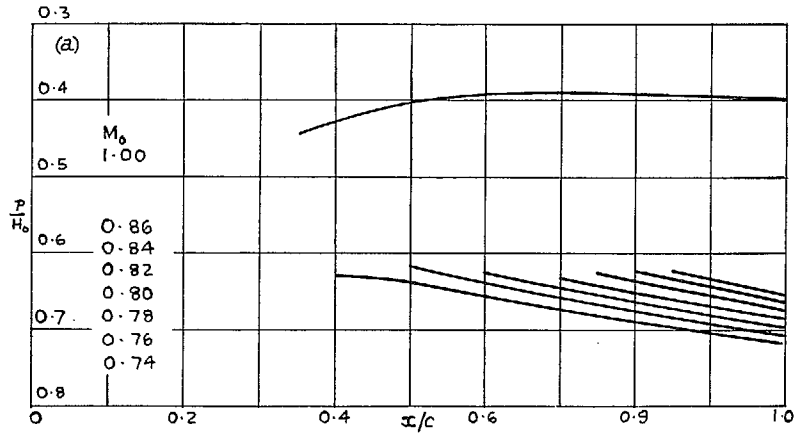

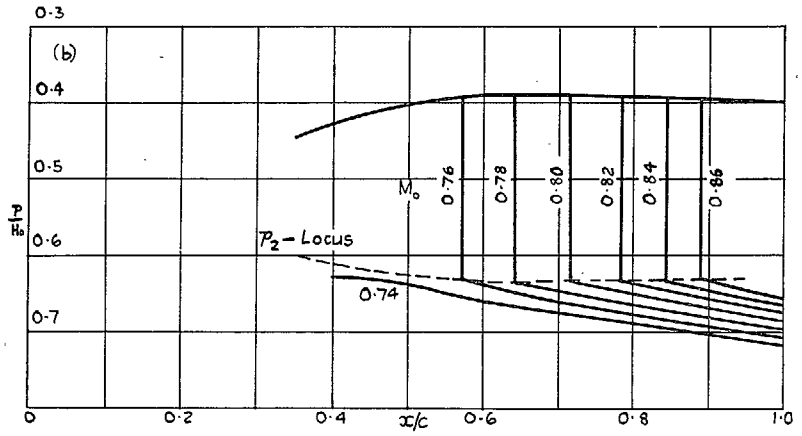

FIGS. 3a and 3b. Basic method for estimating transonic distributions.

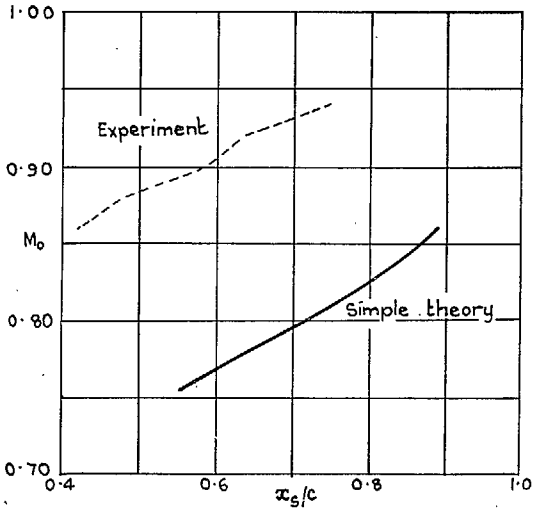

FIG. 4. Comparison of shock positions.

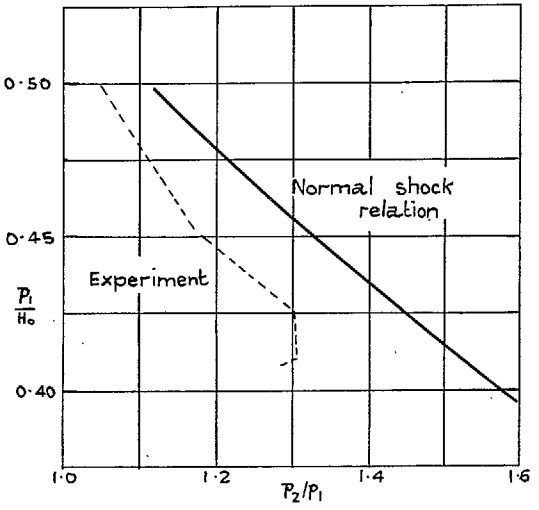

FIG. 5. Comparison of shock pressure rises.

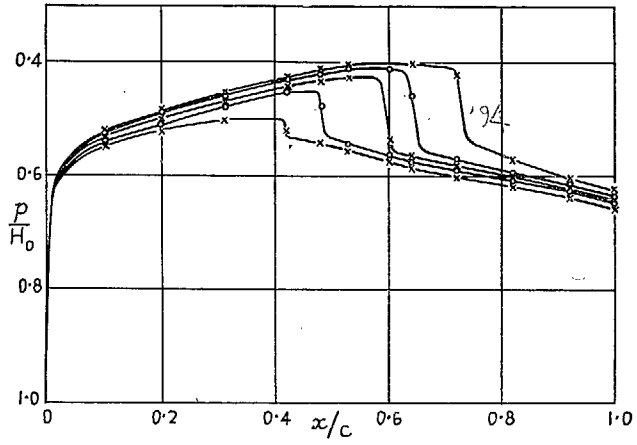

FIG. 6. 6 per cent RAE 102, $\alpha = 0$ deg.
$M_0 = 0{\cdot}86$ to $0{\cdot}94$.

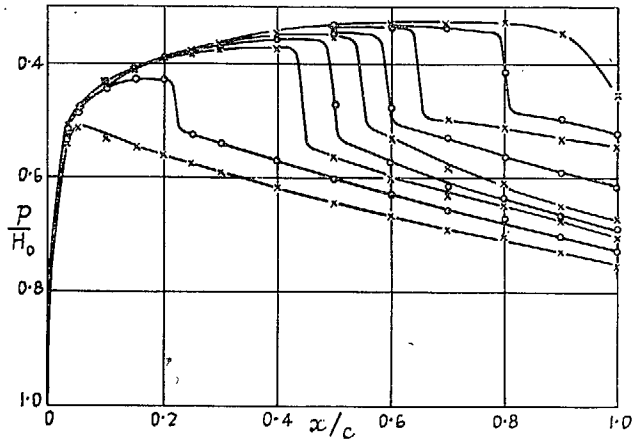

FIG. 7. NACA 0009_5, $\alpha = 2$ deg.
$M_0 = 0{\cdot}70$ to $1{\cdot}00$.

FIGS. 6 and 7. Typical measured transonic pressure distributions.

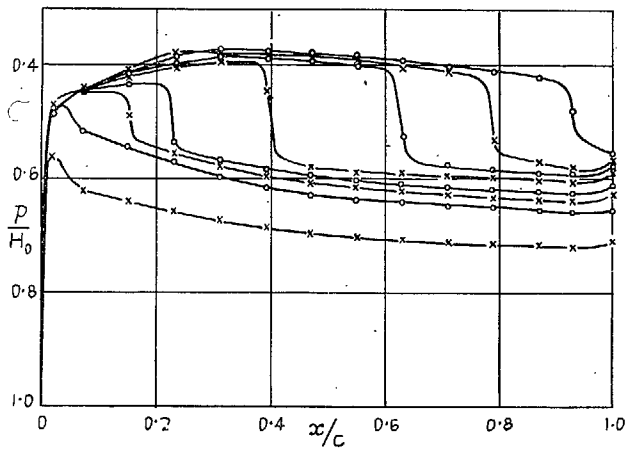

FIG. 8. 4 per cent NPL 491, $\alpha = 1$ deg.
$M_0 = 0{\cdot}70$ to $1{\cdot}00$.

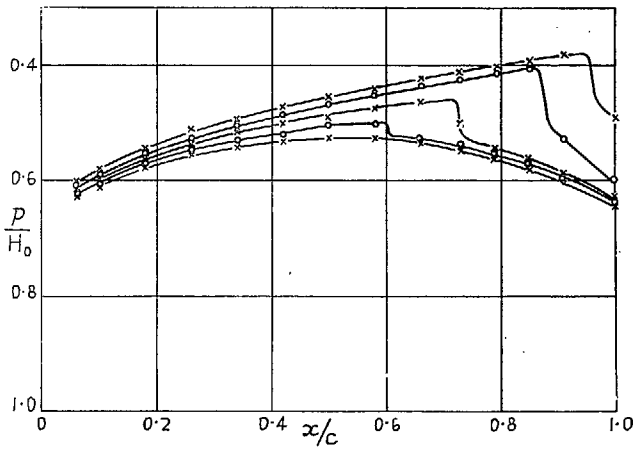

FIG. 9. 4 per cent biconvex aerofoil, $\alpha = 0$ deg.
$M_0 = 0{\cdot}87$ to $1{\cdot}00$.

FIGS. 8 and 9. Typical measured transonic pressure distributions.

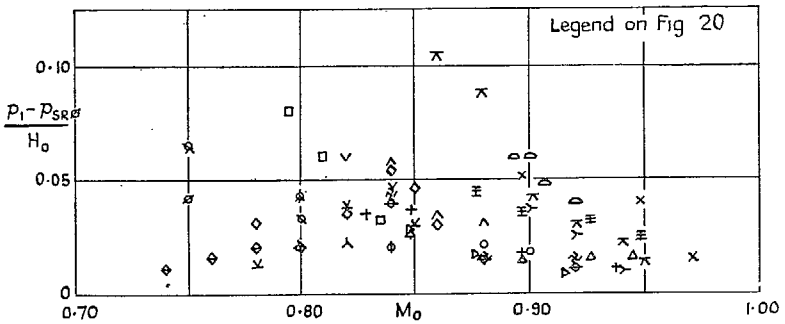

FIG. 10.

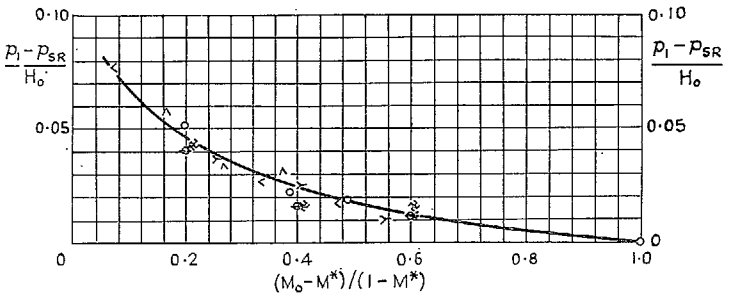

FIG. 11. Values from 1/30th open walls and $\alpha = 0$ deg.

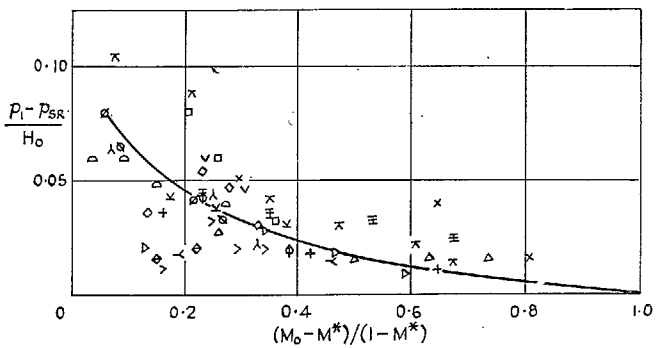

FIG. 12. Other values.

FIGS. 10, 11 and 12. Analysis for p_1/H_0.

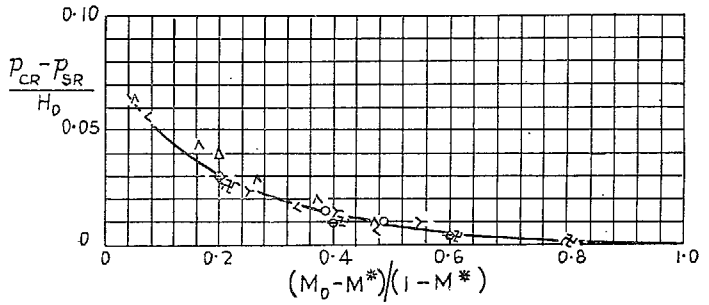

FIG. 13. Values from 1/30th open walls and $\alpha = 0$ deg.

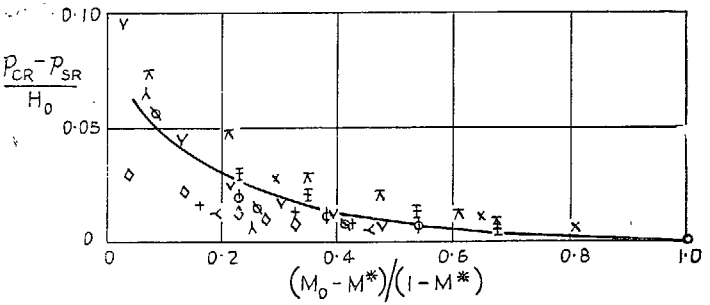

FIG. 14. Other values.

FIGS. 13 and 14. Analysis for p_{CR}/H_0.

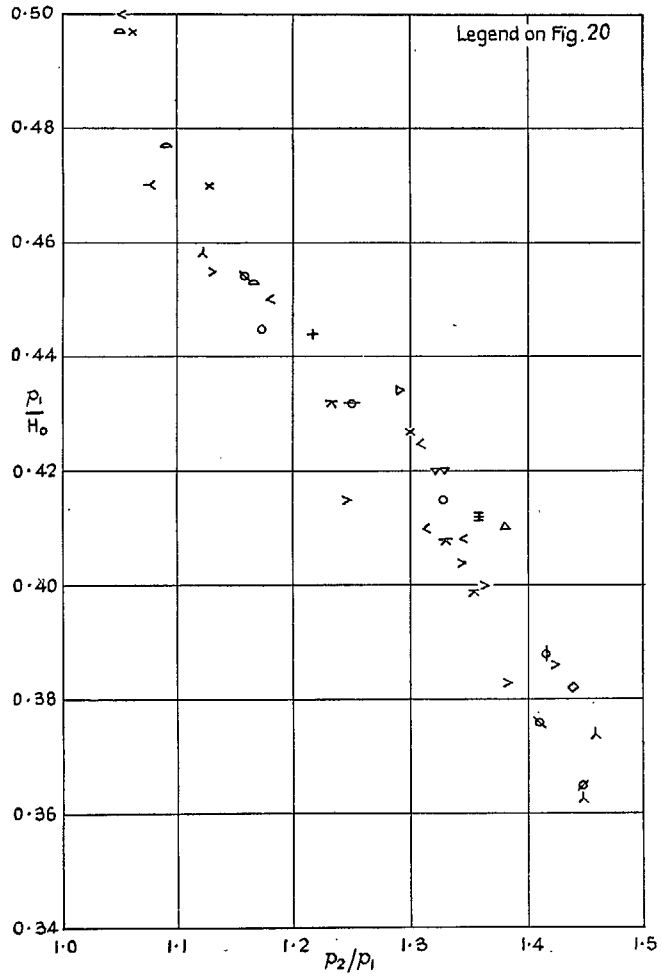

FIG. 15. Measured shock pressure-rise ratio values.

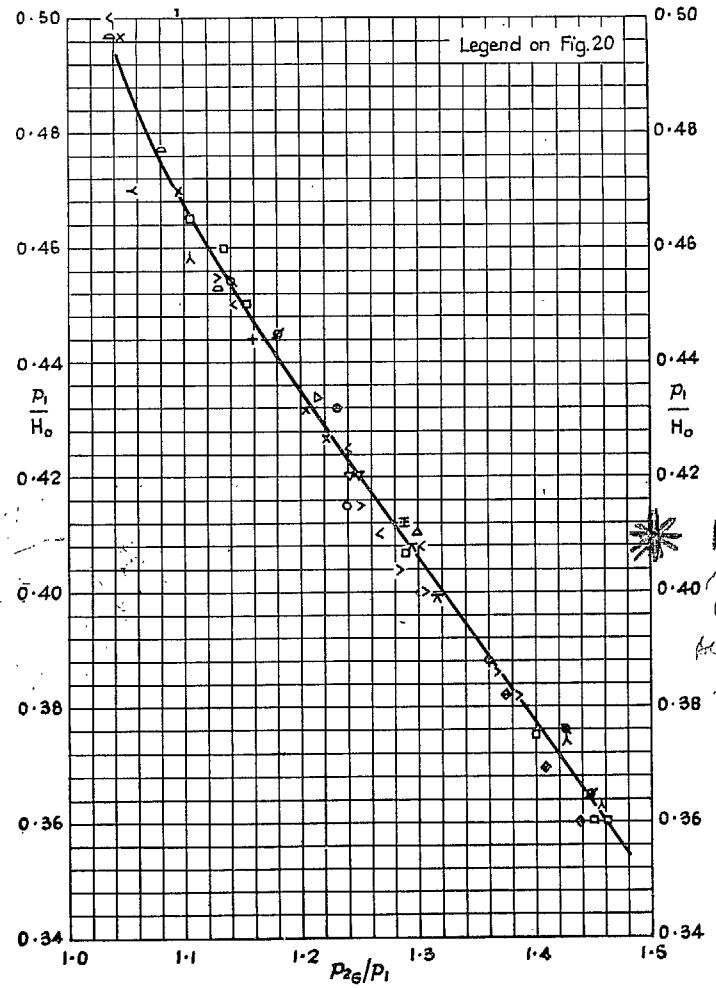

FIG. 16. Empirical shock pressure-rise ratio relation.

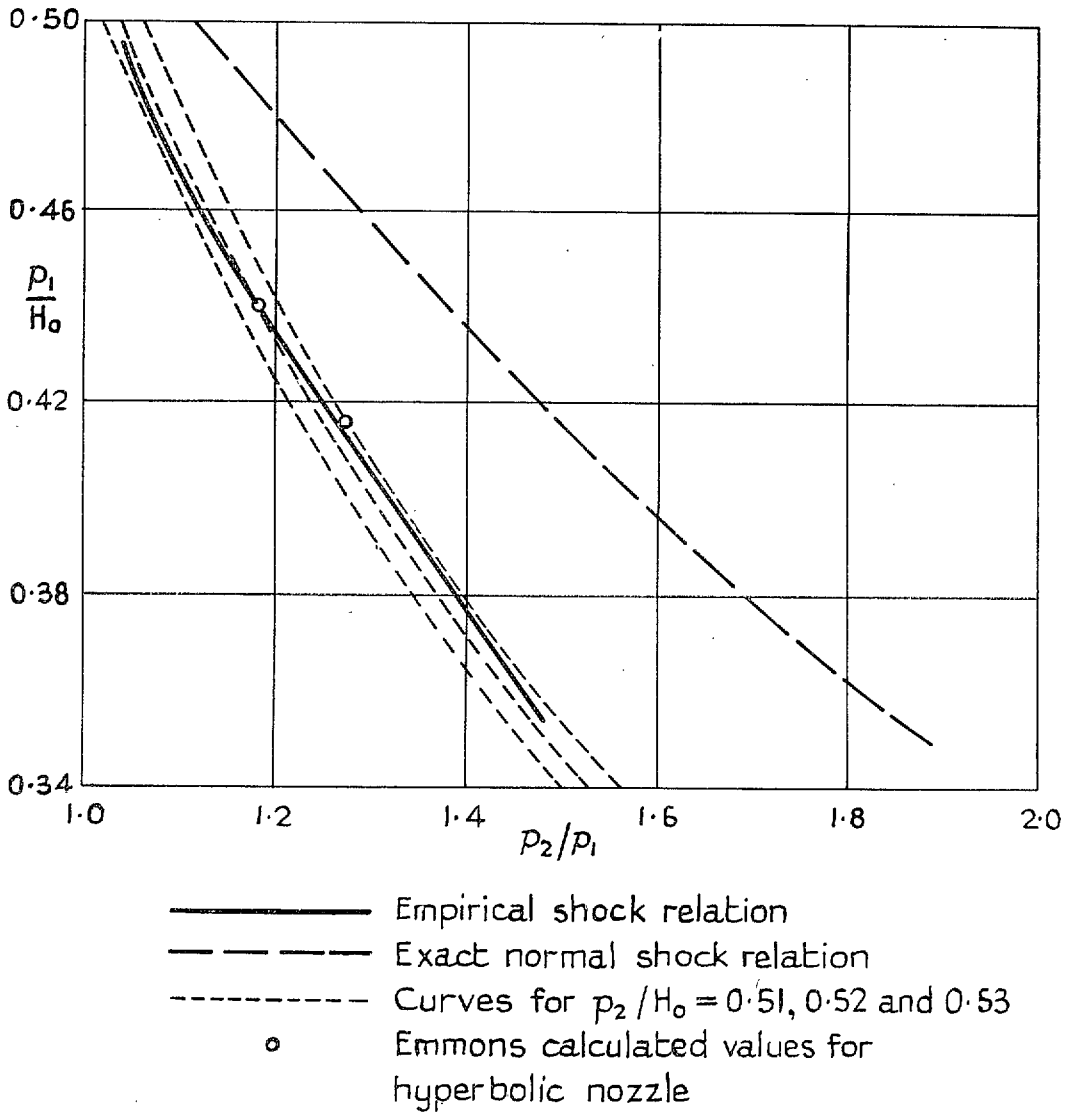

FIG. 17. Comparison of empirical, exact, and constant p_2/H_0 shock relations.

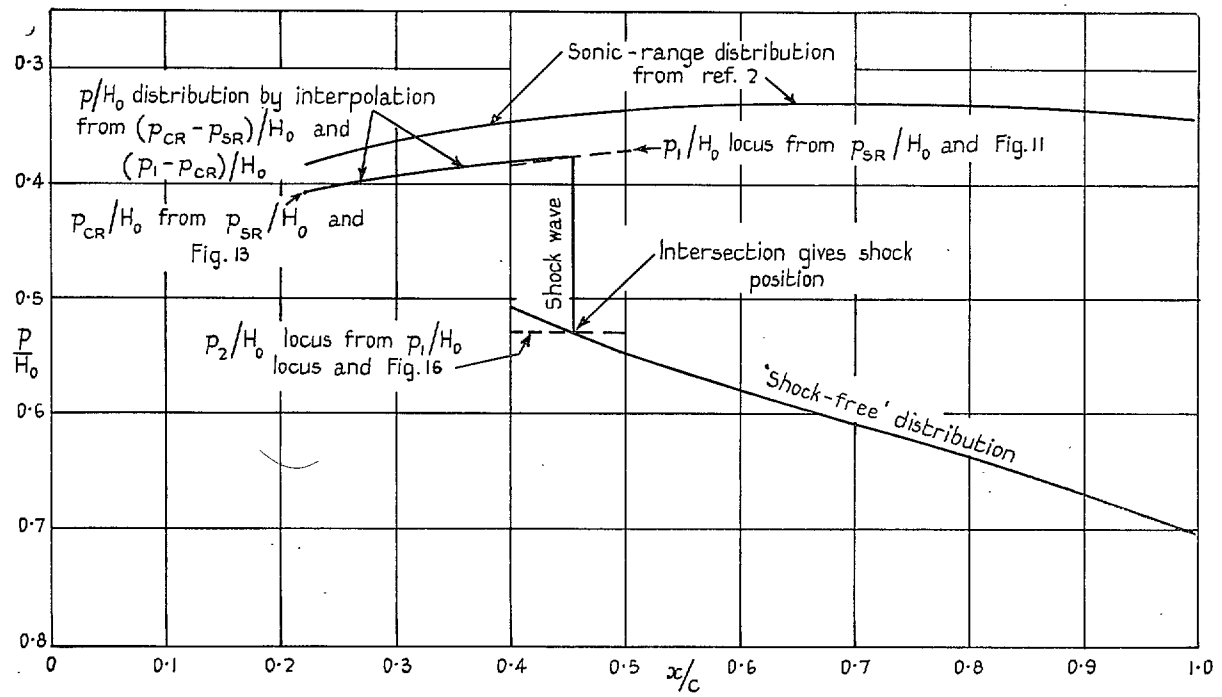

FIG. 18. Illustration of scheme for predicting transonic pressure distributions.

M = 0·80

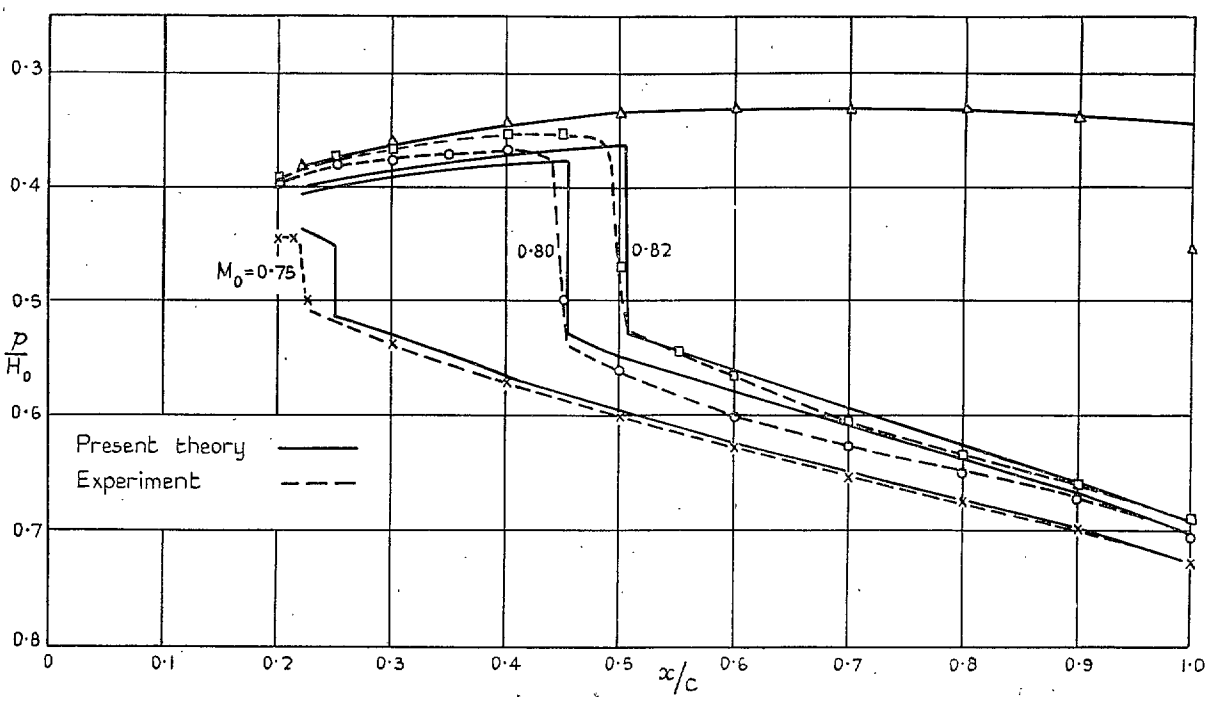

FIG. 19. Comparison of results obtained in Tables 1 to 4 with experiment.

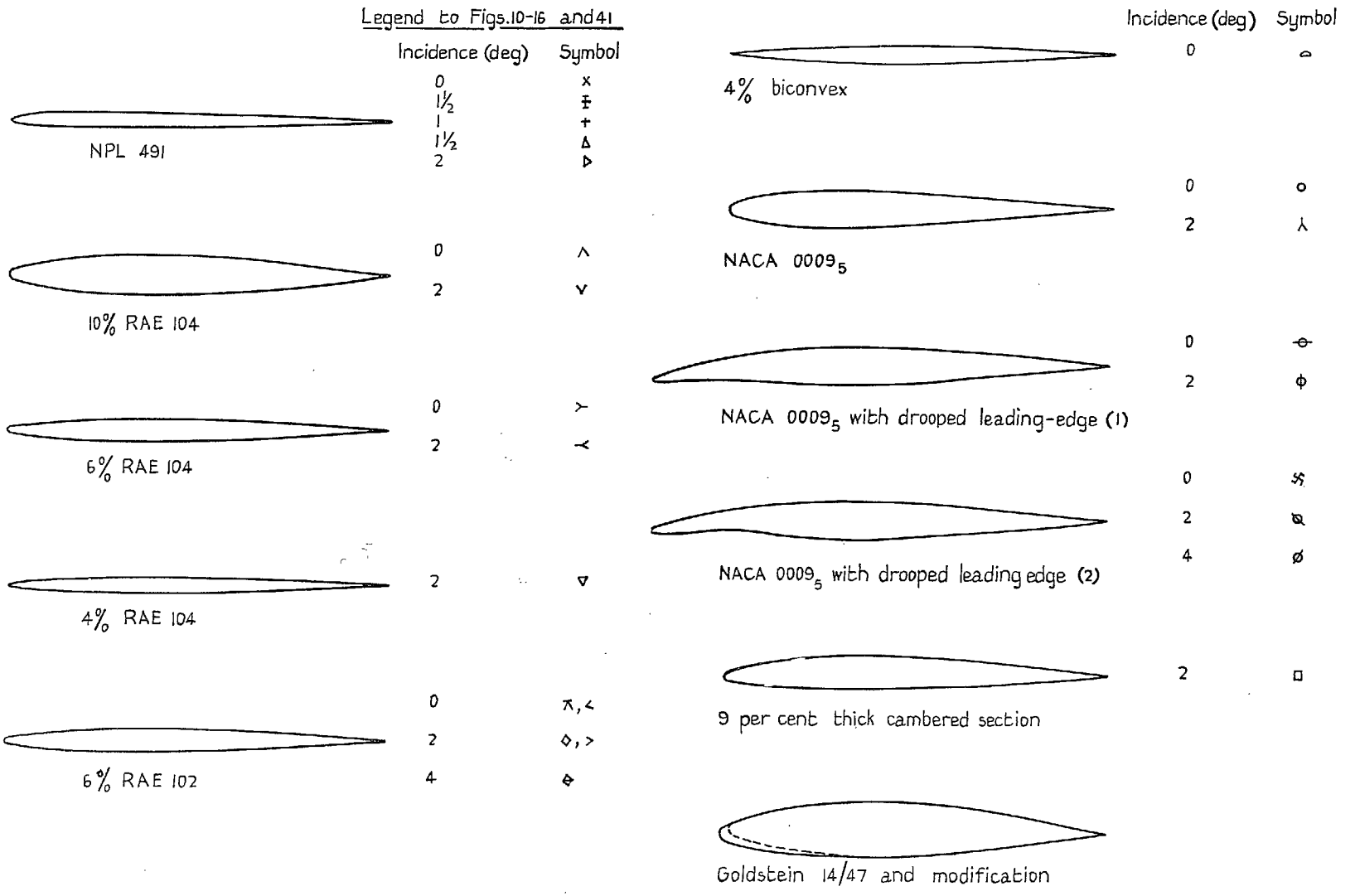

FIG. 20. Profiles of aerofoils used in analysis.

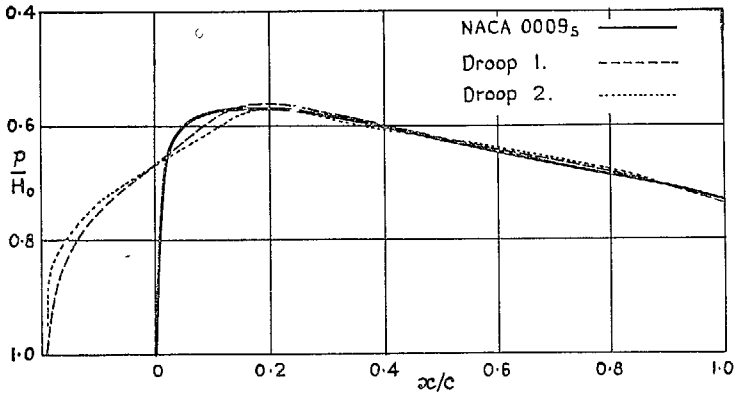

(a) NACA 0009_5 and drooped leading-edge modifications, $M_0 = 0{\cdot}75$, $\alpha = 0$ deg.

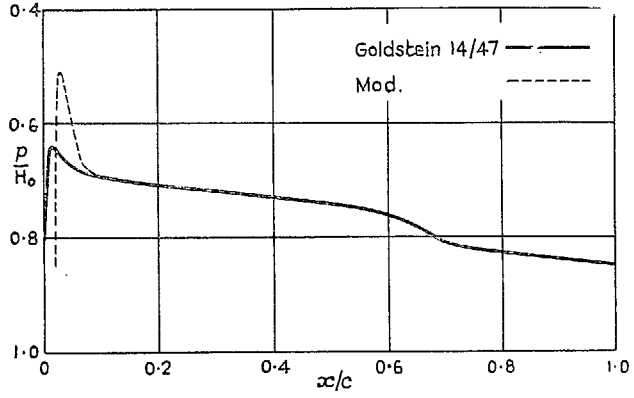

(b) Goldstein 14/47 and modification, $M_0 = 0{\cdot}50$, $\alpha = 5$ deg.

FIGS. 21a and 21b. Effect of leading-edge geometry modifications on pressure distributions.

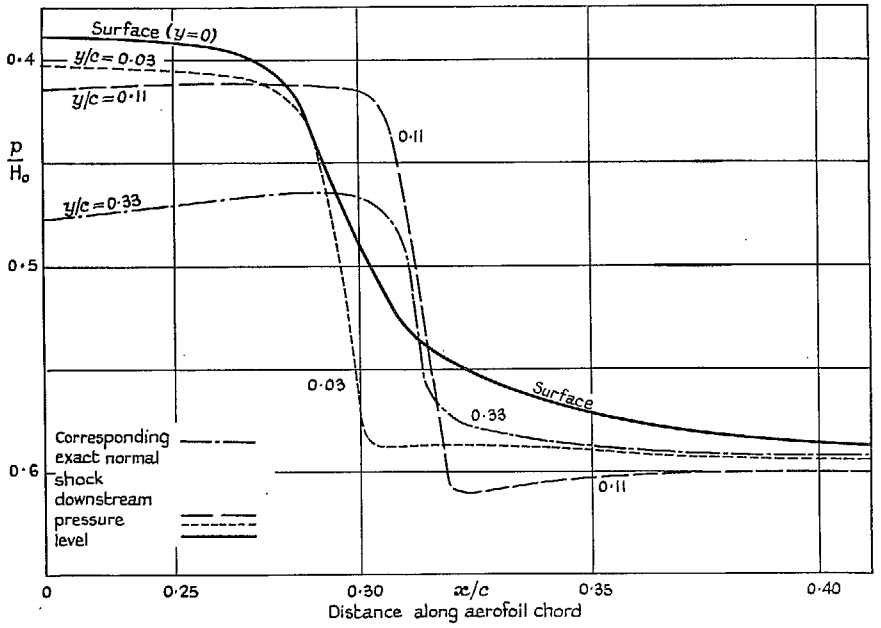

FIG. 22. Pressure distribution on and above the surface of the NPL 491 aerofoil, $\alpha = 1\frac{1}{2}$ deg, $M_0 = 0{\cdot}85$.—Shock at 30 per cent chord.

FIGS. 23—40

COMPARISONS OF CALCULATED AND MEASURED PRESSURE DISTRIBUTIONS

In the following figures calculated pressure distributions are shown by full line curves and experimental results by symbols joined by broken lines to indicate shock position. Free-stream Mach number (x100) is shown on each at the shock position.

Cases not used in the shock pressure rise analysis are distinquished by an asterisk.

The calculated distributions for $M_o = 1 \cdot 0$ were obtained by the method of Ref. 2.

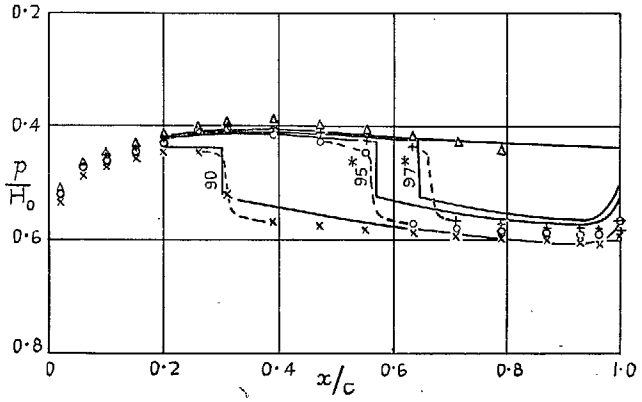

FIG. 23. NPL 491, $\alpha = 0$ deg.

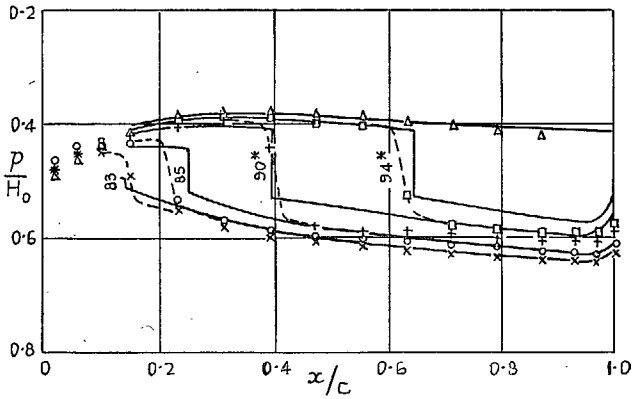

FIG. 24. NPL 491, $\alpha = 1$ deg.

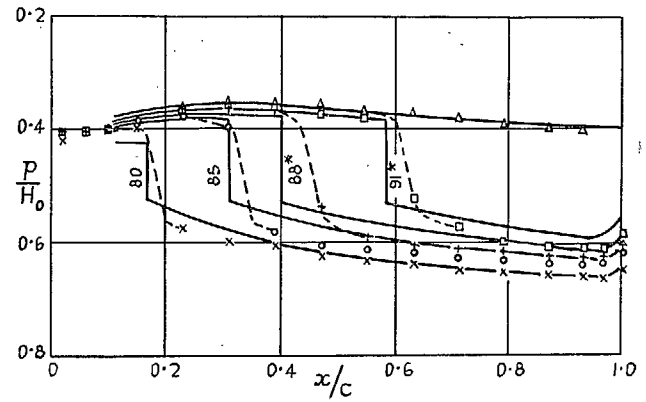

FIG. 25. NPL 491, $\alpha = 2$ deg.

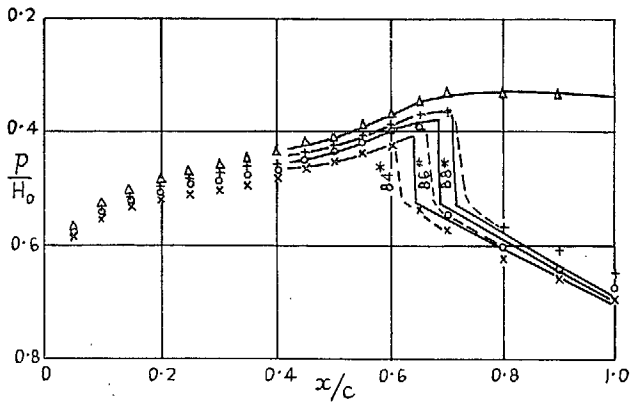

FIG. 26. 10 per cent RAE 104, $\alpha = 0$ deg.

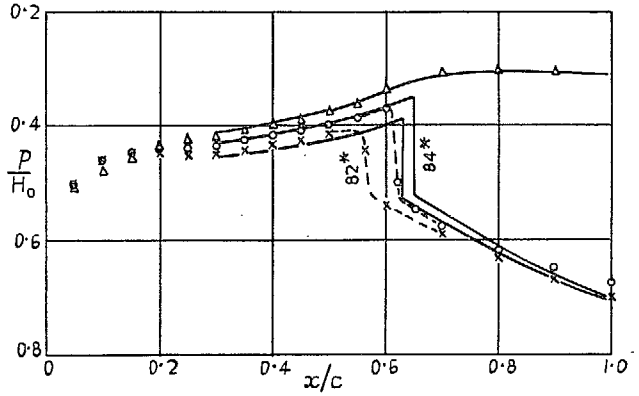

FIG. 27. 10 per cent RAE 104, $\alpha = 2$ deg.

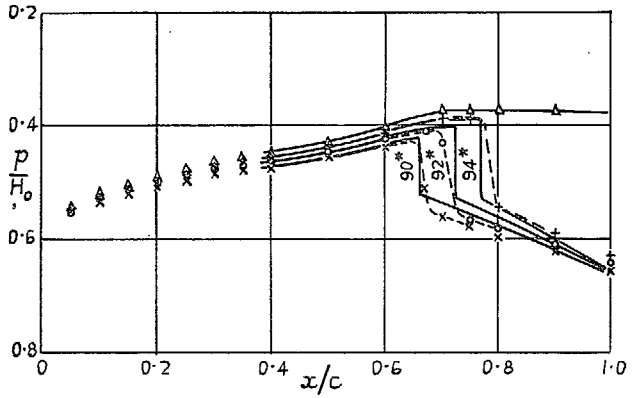

FIG. 28. 6 per cent RAE 104, $\alpha = 0$ deg.

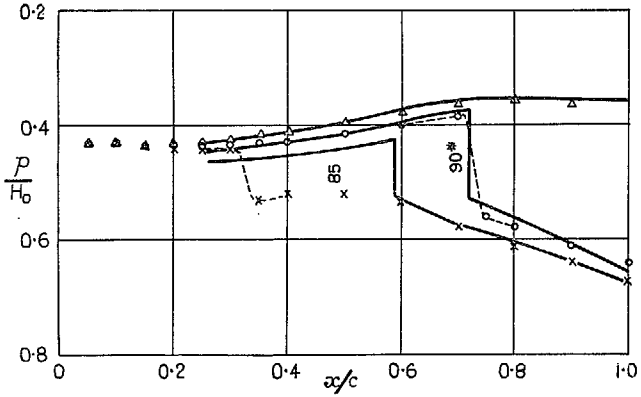

FIG. 29. 6 per cent RAE 104, $\alpha = 2$ deg.

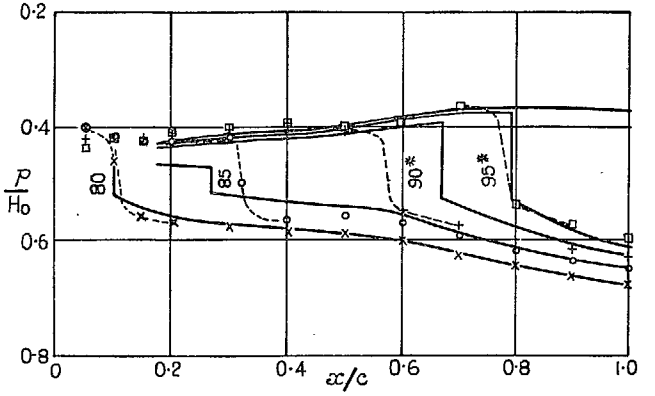

FIG. 30. 4 per cent RAE 104, $\alpha = 2$ deg.

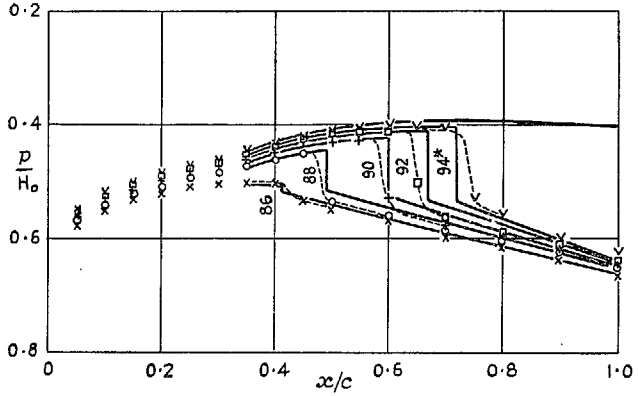

FIG. 31. 6 per cent RAE 102, $\alpha = 0$ deg.

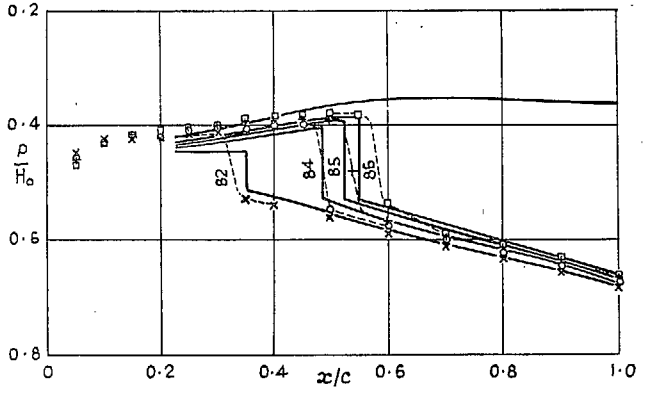

FIG. 32. 6 per cent RAE 102, $\alpha = 2$ deg.

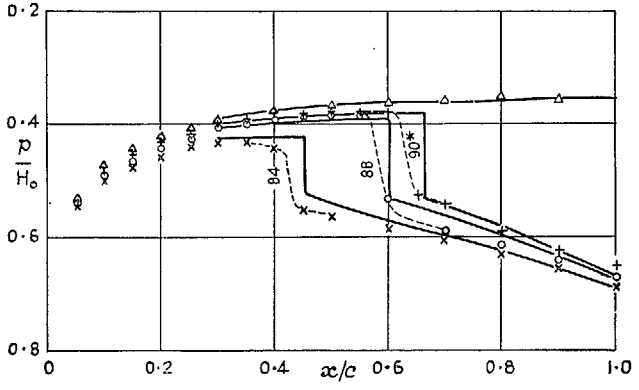

FIG. 33. NACA 0009_5, $\alpha = 0$ deg.

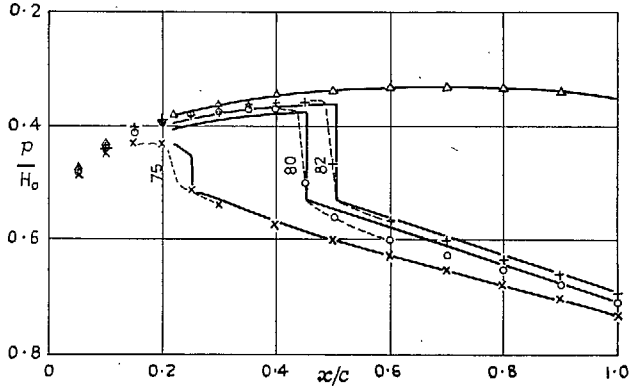

FIG. 34. NACA 0009_5, $\alpha = 2$ deg.

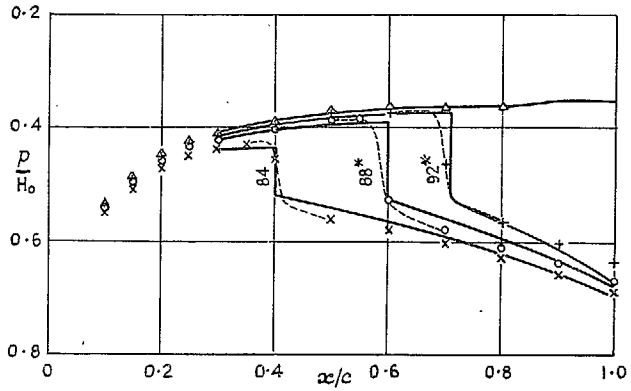

FIG. 35. NACA 0009_5 with droop (1), $\alpha = 0$ deg.

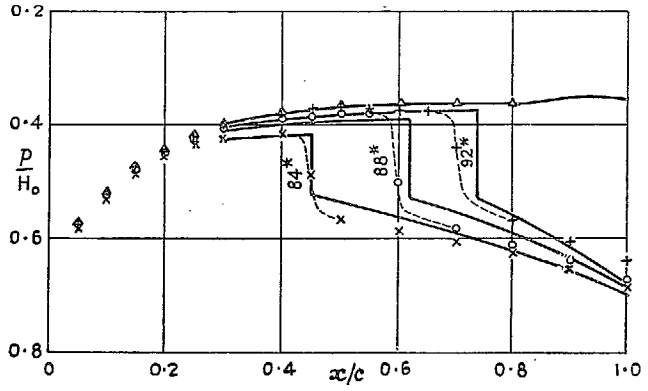

FIG. 37. NACA 0009_5 with droop (2), $\alpha = 0$ deg.

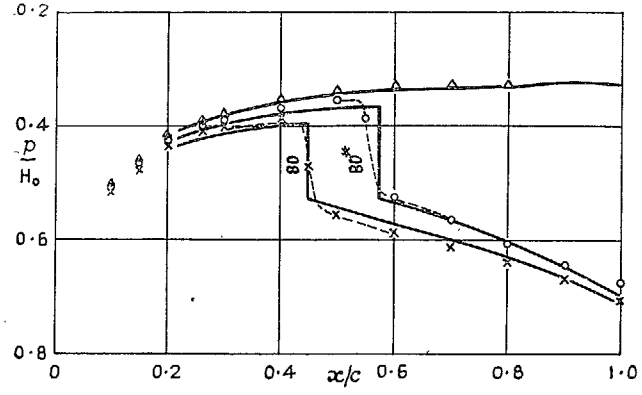

FIG. 36. NACA 0009_5 with droop (1), $\alpha = 2$ deg.

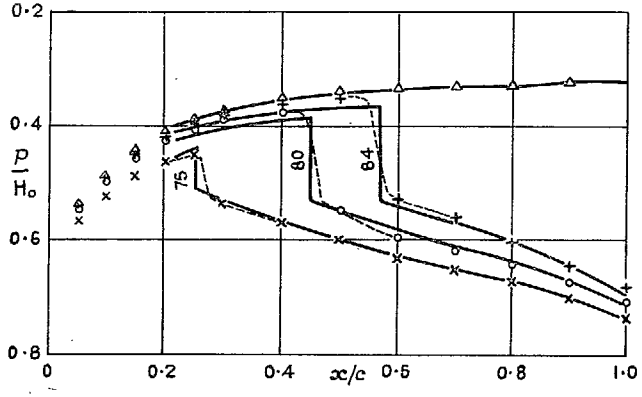

FIG. 38. NACA 0009_5 with droop (2), $\alpha = 2$ deg.

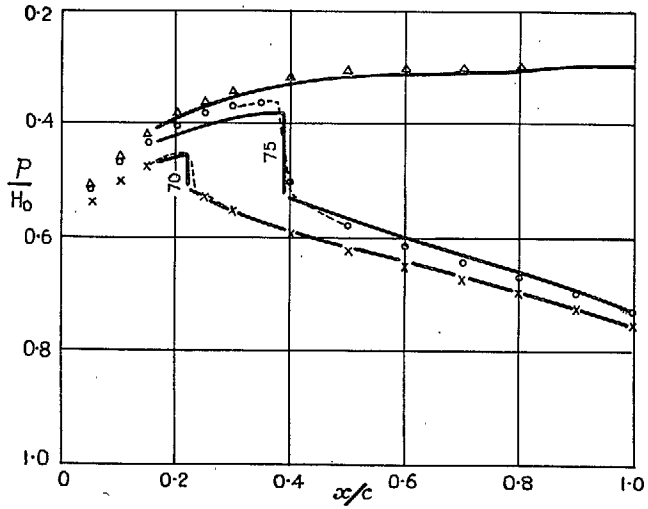

FIG. 39. NACA 0009_5 with droop (2), $\alpha = 4$ deg.

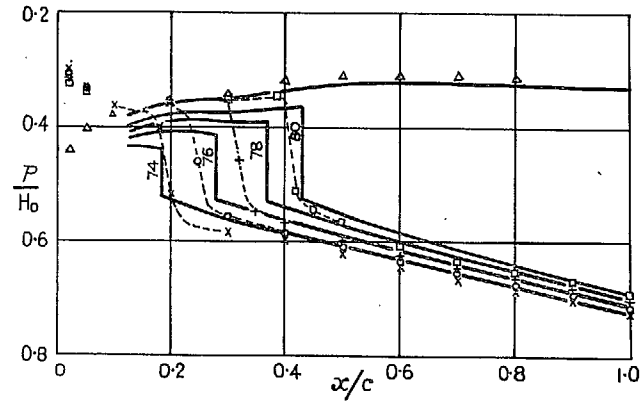

FIG. 40. 6 per cent RAE 102, $\alpha = 4$ deg.

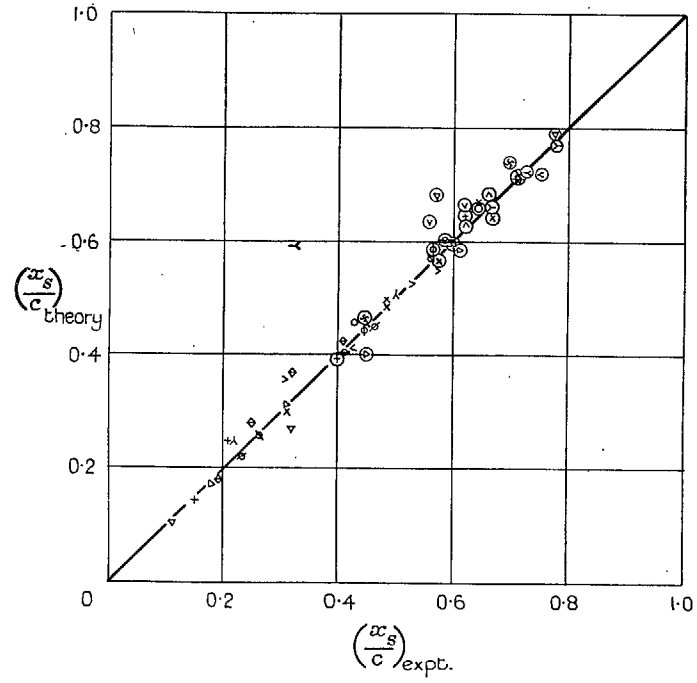

Ringed values not used in analysis for shock pressure rise.

FIG. 41. Direct comparison of calculated and observed shock positions.

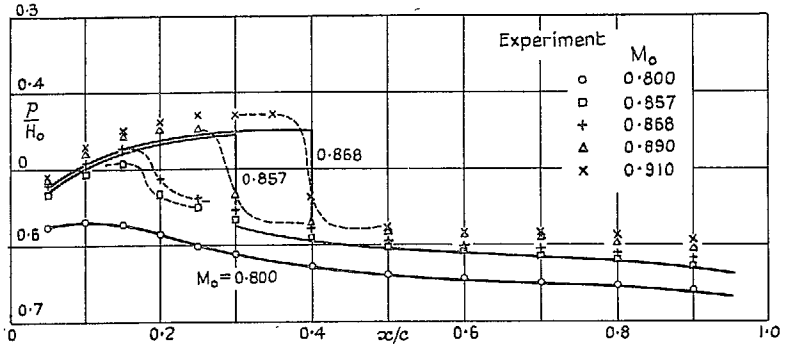

(a) N.P.L. 491 Aerofoil

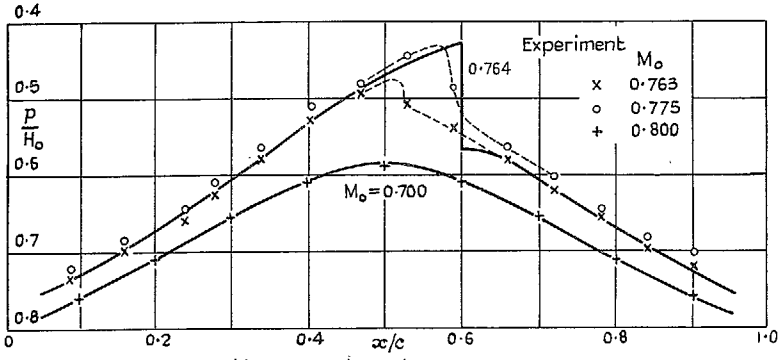

(b) Bi-cusped section

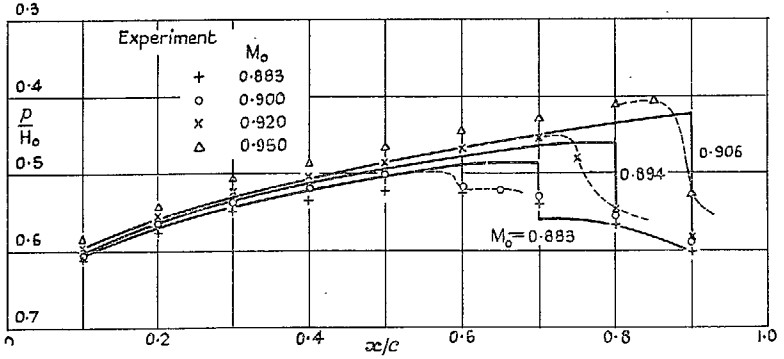

(c) Biconvex section

FIGS. 42a to 42c. Calculated and measured pressure distributions.

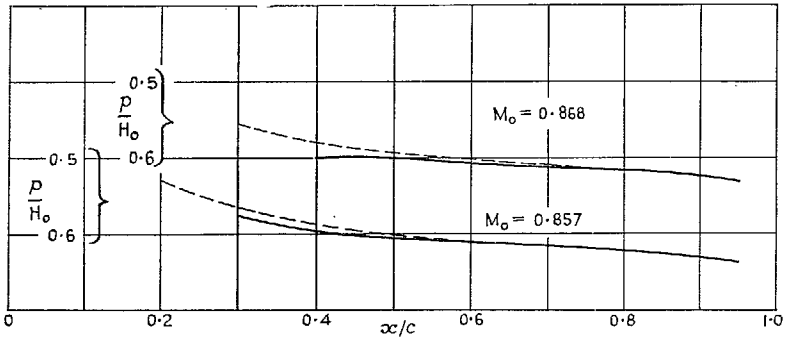

(a) N.P.L. 491 aerofoil

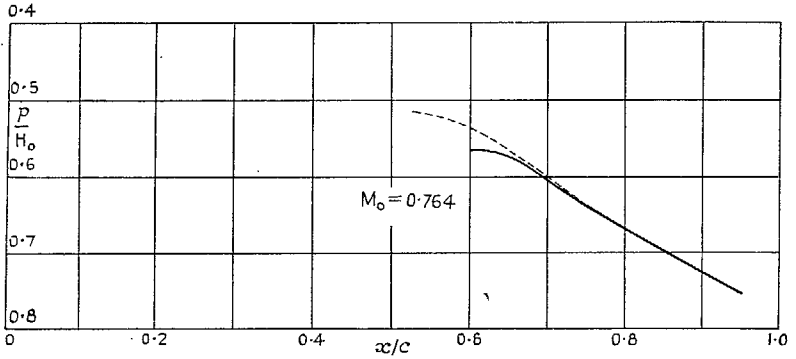

(b) Kaplan Bi-cusped section

Ref. 3 ———
Glauert - - - - - -

FIGS. 43a and 43b. Comparisons of subsonic pressure distributions calculated from Ref. 3 and by Glauert compressibility rule.

(78820) Wt. 54/8210 K.5 8/61 Hw

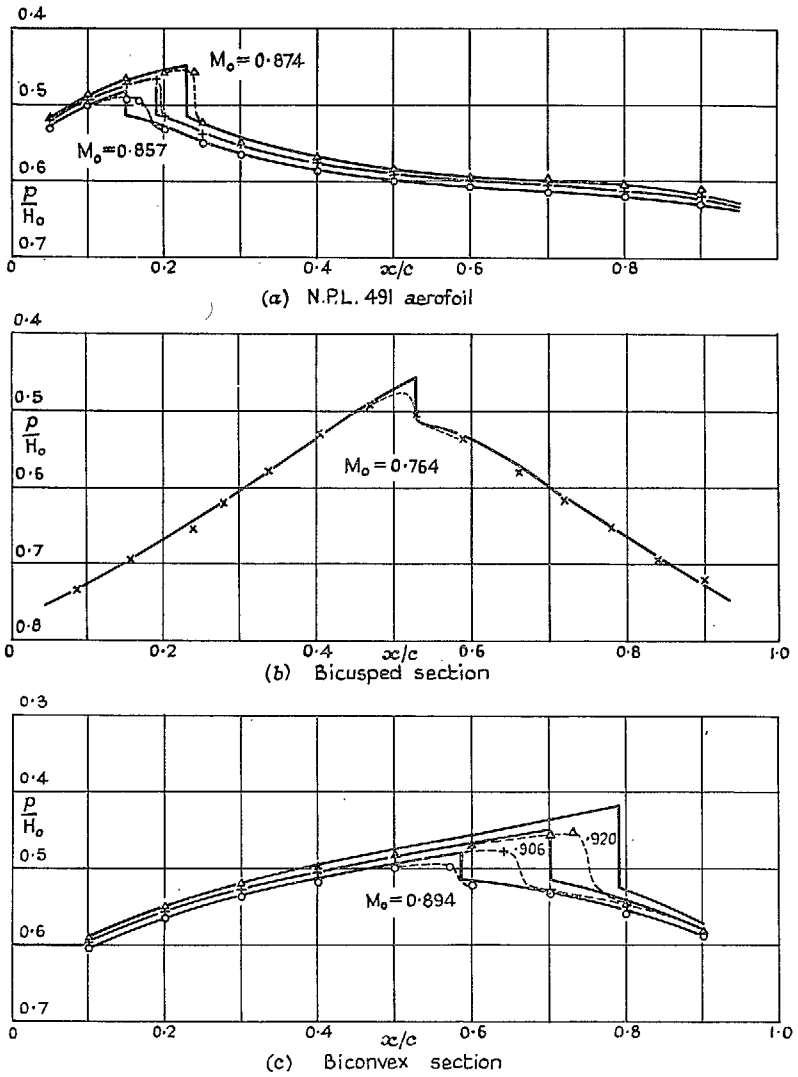

FIGS. 44a to 44c. Comparison of modified theoretical solutions with experiment.

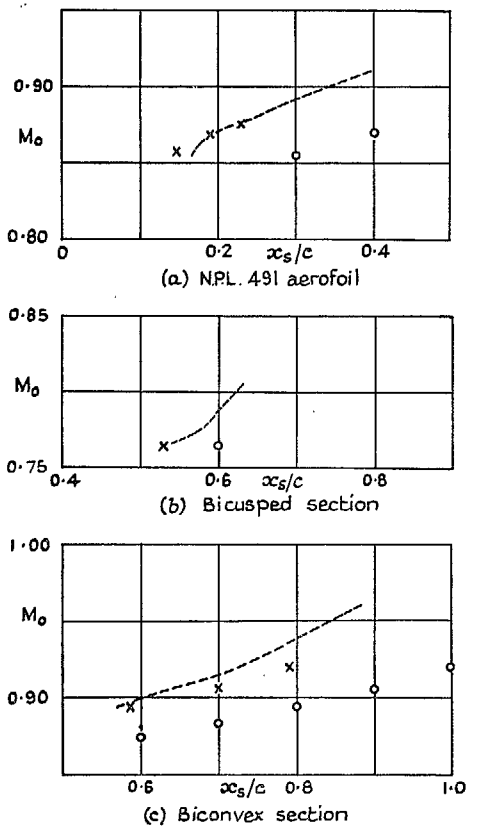

FIGS. 45a to 45c. Comparisons of predicted and measured shock-wave positions.

Publications of the Aeronautical Research Council

ANNUAL TECHNICAL REPORTS OF THE AERONAUTICAL RESEARCH COUNCIL (BOUND VOLUMES)

1941 Aero and Hydrodynamics, Aerofoils, Airscrews, Engines, Flutter, Stability and Control, Structures. 63*s.* (post 2*s.* 3*d.*)

1942 Vol. I. Aero and Hydrodynamics, Aerofoils, Airscrews, Engines. 75*s.* (post 2*s.* 3*d.*)
Vol. II. Noise, Parachutes, Stability and Control, Structures, Vibration, Wind Tunnels. 47*s.* 6*d.* (post 1*s.* 9*d.*)

1943 Vol. I. Aerodynamics, Aerofoils, Airscrews. 80*s.* (post 2*s.*)
Vol. II. Engines, Flutter, Materials, Parachutes, Performance, Stability and Control, Structures. 90*s.* (post 2*s.* 3*d.*)

1944 Vol. I. Aero and Hydrodynamics, Aerofoils, Aircraft, Airscrews, Controls. 84*s.* (post 2*s.* 6*d.*)
Vol. II. Flutter and Vibration, Materials, Miscellaneous, Navigation, Parachutes, Performance, Plates and Panels, Stability, Structures, Test Equipment, Wind Tunnels. 84*s.* (post 2*s.* 6*d.*)

1945 Vol. I. Aero and Hydrodynamics, Aerofoils. 130*s.* (post 3*s.*)
Vol. II. Aircraft, Airscrews, Controls. 130*s.* (post 3*s.*)
Vol. III. Flutter and Vibration, Instruments, Miscellaneous, Parachutes, Plates and Panels, Propulsion. 130*s.* (post 2*s.* 9*d.*)
Vol. IV. Stability, Structures, Wind Tunnels, Wind Tunnel Technique. 130*s.* (post 2*s.* 9*d.*)

1946 Vol. I. Accidents, Aerodynamics, Aerofoils and Hydrofoils. 168*s.* (post 3*s.* 3*d.*)
Vol. II. Airscrews, Cabin Cooling, Chemical Hazards, Controls, Flames, Flutter, Helicopters, Instruments and Instrumentation, Interference, Jets, Miscellaneous, Parachutes. 168s. (post 2*s.* 9*d.*)
Vol. III. Performance, Propulsion, Seaplanes, Stability, Structures, Wind Tunnels. 168*s.* (post 3*s.*)

1947 Vol. I. Aerodynamics, Aerofoils, Aircraft. 168*s.* (post 3*s.* 3*d.*)
Vol. II. Airscrews and Rotors, Controls, Flutter, Materials, Miscellaneous, Parachutes, Propulsion, Seaplanes, Stability, Structures, Take-off and Landing. 168*s.* (post 3*s.* 3*d.*)

Special Volumes

Vol. I. Aero and Hydrodynamics, Aerofoils, Controls, Flutter, Kites, Parachutes, Performance, Propulsion, Stability. 126*s.* (post 2*s.* 6*d.*)
Vol. II. Aero and Hydrodynamics, Aerofoils, Airscrews, Controls, Flutter, Materials, Miscellaneous, Parachutes, Propulsion, Stability, Structures. 147*s.* (post 2*s.* 6*d.*)
Vol. III. Aero and Hydrodynamics, Aerofoils, Airscrews, Controls, Flutter, Kites, Miscellaneous, Parachutes, Propulsion, Seaplanes, Stability, Structures, Test Equipment. 189*s.* (post 3*s.* 3*d.*)

Reviews of the Aeronautical Research Council

1939–48 3*s.* (post 5*d.*) 1949–54 5*s.* (post 5*d.*)

Index to all Reports and Memoranda published in the Annual Technical Reports

1909–1947 R. & M. 2600 6*s.* (post 2*d.*)

Indexes to the Reports and Memoranda of the Aeronautical Research Council

Between Nos. 2351–2449	R. & M. No. 2450 2*s.* (post 2*d.*)
Between Nos. 2451–2549	R. & M. No. 2550 2*s.* 6*d.* (post 2*d.*)
Between Nos. 2551–2649	R. & M. No. 2650 2*s.* 6*d.* (post 2*d.*)
Between Nos. 2651–2749	R. & M. No. 2750 2*s.* 6*d.* (post 2*d.*)
Between Nos. 2751–2849	R. & M. No. 2850 2*s.* 6*d.* (post 2*d.*)
Between Nos. 2851–2949	R. & M. No. 2950 3*s.* (post 2*d.*)
Between Nos. 2951–3049	R. & M. No. 3050 3*s.* 6*d.* (post 2*d.*)

HER MAJESTY'S STATIONERY OFFICE

from the addresses overleaf

Printed and published by
HER MAJESTY'S STATIONERY OFFICE

To be purchased from
York House, Kingsway, London W.C.2
423 Oxford Street, London W.1
13A Castle Street, Edinburgh 2
109 St. Mary Street, Cardiff
39 King Street, Manchester 2
50 Fairfax Street, Bristol 1
2 Edmund Street, Birmingham 3
80 Chichester Street, Belfast 1
or through any bookseller

Printed in England

S.O. Code No. 23-3156